

\mathbb{R} -MOTIVIC v_1 -PERIODIC HOMOTOPY

EVA BELMONT, DANIEL C. ISAKSEN, AND HANA JIA KONG

ABSTRACT. We compute the v_1 -periodic \mathbb{R} -motivic stable homotopy groups. The main tool is the effective slice spectral sequence. Along the way, we also analyze \mathbb{C} -motivic and η -periodic v_1 -periodic homotopy from the same perspective.

1. INTRODUCTION

The computation of the stable homotopy groups of spheres is a difficult but central problem of stable homotopy theory. There is much that we do not know about stable homotopy. However, the v_1 -periodic stable homotopy groups (also known for historical reasons as the image of j) are completely understood, and they have interesting number-theoretic properties.

The goal of this article is to explore v_1 -periodic stable homotopy in the \mathbb{R} -motivic context. This choice of ground field represents a middle ground between the well-understood \mathbb{C} -motivic situation and the much more difficult situation of an arbitrary field, in which arithmetic necessarily enters into the picture.

From our perspective, the field \mathbb{R} introduces just one piece of arithmetic: the failure of -1 to have a square root. This leads to complications in \mathbb{R} -motivic homotopical computations, but they can be managed with care and attention to detail.

Classically, v_1 -periodic homotopy is detected by the connective spectrum j^{top} , which is defined to be the fiber of a map $\text{ko}^{\text{top}} \xrightarrow{\psi^3 - 1} \Sigma^4 \text{ksp}^{\text{top}}$, where ko^{top} is the connective real K -theory spectrum, ksp^{top} is the connective symplectic K -theory spectrum, and ψ^3 is an Adams operation. (The “top” superscripts indicate that we are discussing the classical context here, rather than the motivic context.)

In fact, ko^{top} itself is the more natural target for the map $\psi^3 - 1$. However, the fiber of $\text{ko}^{\text{top}} \xrightarrow{\psi^3 - 1} \text{ko}^{\text{top}}$ has a minor defect. It has some additional homotopy classes in stems -1 , 0 , and 1 that do not correspond to homotopy classes for the sphere spectrum. In other words, the map from S^0 to this fiber is not surjective in homotopy. If we change the target of $\psi^3 - 1$ from ko^{top} to its connective cover $\Sigma^4 \text{ksp}^{\text{top}}$, then this problem disappears, and the map from S^0 to the fiber is onto in homotopy.

2010 *Mathematics Subject Classification*. Primary 55Q10; Secondary 14F42, 55Q51, 55T99.

Key words and phrases. motivic stable homotopy group, v_1 -periodicity, effective spectral sequence.

The second author was supported by NSF grant DMS-1904241. The third author was supported by the National Science Foundation under Grant No. DMS-1926686. This manuscript answers a question posed by Mark Behrens to the second author in 2010 at the Conference on Homotopy Theory and Derived Algebraic Geometry, Fields Institute, Toronto, Ontario, Canada. The authors thank William Balderrama, Robert Bruner, and John Rognes for helpful discussions.

It is possible to mimic these constructions in motivic stable homotopy theory [BH20]. At the prime 2, one can define the motivic connective spectrum j to be the fiber of a map $\mathrm{ko} \xrightarrow{\psi^3-1} \Sigma^{4,2}\mathrm{ksp}$, where ko is the very effective connective Hermitian K -theory spectrum, ksp is defined in terms of very effective covers of ko , and ψ^3 is a motivic lift of an Adams operation.

However, from a computational perspective, this definition of j introduces apparently unnecessary complications. It is possible to compute the homotopy of \mathbb{R} -motivic j using the techniques that appear later in this manuscript. However, the computation is slightly messy, involving some exceptional differentials and exceptional hidden extensions in low dimensions. In any case, the homotopy of the \mathbb{R} -motivic sphere does not surject onto the homotopy of \mathbb{R} -motivic j . In other words, the main rationale for using ksp in the first place does not apply in the motivic situation.

On the other hand, the computation of the homotopy of the \mathbb{R} -motivic fiber of $\mathrm{ko} \xrightarrow{\psi^3-1} \mathrm{ko}$ is much cleaner. Moreover, it tells us just as much about v_1 -periodic \mathbb{R} -motivic homotopy as j . In other words, it has all of the computational advantages of j , while avoiding some unfortunate complications.

Consequently, in this manuscript, we will be solely concerned with the fiber of $\mathrm{ko} \xrightarrow{\psi^3-1} \mathrm{ko}$. We use the notation L for this fiber in order to avoid confusion with the traditional meaning of j . The symbol L is meant to draw a connection to the classical $K(1)$ -local sphere $L_{K(1)}S^0$, which is the fiber of $\mathrm{KO}^{\mathrm{top}} \xrightarrow{\psi^3-1} \mathrm{KO}^{\mathrm{top}}$.

However, the homotopy of the \mathbb{R} -motivic spheres does not surject onto the homotopy of \mathbb{R} -motivic L . It is possible that we may have not yet constructed the “correct” motivic version of the classical connective spectrum j^{top} . These considerations raise questions about vector bundles and the motivic Adams conjecture. We make no attempt to study these more geometric issues.

We claim to compute the v_1 -periodic \mathbb{R} -motivic stable homotopy groups, but this claim deserves some clarification. We do not use an intrinsic definition of v_1 -periodic \mathbb{R} -motivic homotopy, although such a definition could probably be formulated in terms of the motivic $K(1)$ -local sphere. However, the theory of motivic $K(1)$ -localization has not yet been suitably developed.

Rather, we merely compute the homotopy of L , and we observe that it detects large-scale structure in the stable homotopy of the \mathbb{R} -motivic sphere, which was described in a range in [BI20]. In other words, we have a practical description of \mathbb{R} -motivic v_1 -periodic homotopy, not a theoretical one.

The careful reader may object that our approach with effective spectral sequences is long-winded and unnecessarily complicated. In fact, the homotopy of L could be determined by direct analysis of the long exact sequence associated to the defining fiber sequence for L . However, there is a disadvantage in this direct approach. We find that the effective filtration is useful additional information about the homotopy of L that helps us understand the computation. The effective filtration is part of the “higher structure” of the homotopy of L . While we have no immediate uses for this higher structure, we know from experience that it inevitably becomes important in deeper homotopical analyses.

1.1. Charts. We provide a series of charts that display the effective spectral sequences for ko and L , as well as their \mathbb{C} -motivic counterparts. We consider these charts to be the central achievement of this manuscript. We encourage the reader to rely heavily on the charts. In a sense, they provide an illustrated guide to our computations.

Caution must be exercised in the comparison to [BI20] since the Adams filtrations and effective filtrations are different. As in [BI20], our charts consider each coweight separately; we have found that this is a practical way of studying \mathbb{R} -motivic homotopy groups. Periodicity by τ^4 (which is not a permanent cycle, but should be thought of as a periodicity operator in coweight 4) allows us to give a fairly compact depiction of the homotopy of L in coweights congruent to 0, 1, and 2 modulo 4; see Figures 13, 14, and 15.

The homotopy of L in coweights congruent to 3 modulo 4 is much more interesting but harder to describe. See Figures 17 and 18.

1.2. Completions. We are computing exclusively in the 2-complete context. This simplifies all questions surrounding convergence of spectral sequences. Also, the final computational 2-complete answers are easier to state than their 2-localized or integral counterparts.

We generally omit completions from our notation for brevity. For example, we write \mathbb{Z} for the 2-adic integers, and we write KO for the 2-completed \mathbb{R} -motivic Hermitian K -theory spectrum.

Section 2.3 discusses these topics in slightly more detail.

1.3. Regarding the element 2. When passing from the effective E_∞ -page to stable homotopy groups, one must choose homotopy elements that are represented by each element of the E_∞ -page. For the element 2 in the E_∞ -page, there is more than one choice in $\pi_{0,0}$ because of the presence of elements in the E_∞ -page in higher effective filtration.

From the perspective of abelian groups, the element $2 = 1 + 1$ is the obvious choice of homotopy element. However, there is another element \mathfrak{h} , also detected by 2 in the effective spectral sequence, that turns out to be a much more convenient choice. The difference between \mathfrak{h} and 2 in homotopy is detected by the element ρh_1 in higher filtration (to be discussed later). Experience has shown that the motivic stable homotopy groups are easier to describe in terms of \mathfrak{h} than in terms of 2. For example, we have the relations $\mathfrak{h}\rho = 0$ and $\mathfrak{h}\eta = 0$, where ρ and η are the homotopy elements detected by ρ and h_1 respectively. However, neither 2ρ nor 2η are zero.

There are two additional reasons why the element \mathfrak{h} plays a central role. First, it corresponds to the hyperbolic plane under the isomorphism between motivic $\pi_{0,0}$ and the Grothendieck–Witt group of symmetric bilinear forms [Mor04]. Second, it plays the role of the zeroth Hopf map, in the sense that the Steenrod operations on its cofiber are simpler than the Steenrod operations for the cofiber of 2.

Consequently, instead of describing motivic stable homotopy groups as a module over the 2-adic integers \mathbb{Z}_2 (i.e., in terms of the action of 2), it is easier to describe the homotopy groups in terms of the action of \mathfrak{h} .

1.4. Future directions. Our work points toward several open problems.

Problem 1.1. Compute motivic v_1 -periodic homotopy over an arbitrary base field. See Section 1.5 for further discussion.

Problem 1.2. Recompute the homotopy of L using the \mathbb{R} -motivic Adams spectral sequence. This would be a useful comparison object for further computations with the Adams spectral sequence for the \mathbb{R} -motivic sphere. The classical Adams spectral sequence for j^{top} was studied by Davis [Dav75], but it was only recently computed completely by Bruner and Rognes [BR21]. We are proposing a motivic analogue of their results.

Problem 1.3. Carry out the effective spectral sequence for the \mathbb{R} -motivic sphere in a range. These computations would serve as a useful companion to \mathbb{R} -motivic Adams spectral sequence computations [BI20]. The idea is to build on the techniques that are developed in this manuscript.

Problem 1.4. Compute the v_1 -periodic C_2 -equivariant stable homotopy groups. More precisely, carry out the C_2 -effective spectral sequence for a C_2 -equivariant version of L . The details will be similar to but more complicated than the computations in this manuscript. See [Kon21] for the effective approach to the C_2 -equivariant version of ko . Alternatively, one might compute the v_1 -periodic C_2 -equivariant stable homotopy groups by periodicizing the v_1 -periodic \mathbb{R} -motivic groups with respect to τ , as considered by Behrens and Shah [BS20].

Recall that the \mathbb{R} -motivic and C_2 -equivariant stable homotopy groups are isomorphic in a range [BGI21]. Consequently, we anticipate that some version of the structure described in this manuscript appears in the C_2 -equivariant context as well.

In the equivariant context, we mention Balderrama's [Bal21] computation of the homotopy groups of the Borel C_2 -equivariant $K(1)$ -local sphere, using techniques that are entirely different from ours. Roughly speaking, Balderrama computes the $\tau^4 v_1^4$ -periodicization of our result.

Problem 1.5. Study $K(1)$ -localization in the motivic context, which ought to be something like localization with respect to $KGL/2$. Compute $K(1)$ -local motivic homotopy. This would provide an intrinsic definition of v_1 -periodic homotopy that would improve upon the practical computational perspective of this manuscript.

A guide to the motivic situation could lie in the work of Balderrama [Bal21] and Carrick [Car19] on equivariant localizations.

1.5. Towards v_1 -periodic homotopy over general base fields. Our explicit computations point the way towards a complete computation of the v_1 -periodic motivic stable homotopy groups over arbitrary fields. The situation here is analogous to the η -periodic \mathbb{R} -motivic computations of [GI16], which foreshadowed the more general η -periodic computations of [Wil18], [OR20], and [BH20].

Problem 1.6. Let k be an arbitrary field of characteristic different from 2. Let $GW(k)$ be the Grothendieck–Witt ring of symmetric bilinear forms over k . Describe the 2-primary homotopy groups of the k -motivic spectrum L in terms of the cokernels and kernels of multiplication by various powers of 2 and of h on $GW(k)$.

Problem 1.6 is stated only in terms of 2-primary computations because that is the most interesting part. We expect that the generalization to odd primes is straightforward.

The exact powers of 2 and h that are required in Problem 1.6 depend not only on the coweight but also on the stem. Figures 17 and 18 show that $2^{v(j)+3}$ is the relevant power of 2 in most stems in coweight $4j - 1$. Here $v(j)$ is the 2-adic valuation of j , i.e., largest number v such that 2^v divides j . In coweight $4j - 1$ and stem $4i - 1$, we see larger powers of 2, as well as powers of h .

Similar observations apply to the kernels that contribute to coweight $4i$.

1.6. Outline. Section 2 contains some background information that we will need to get started on our computations. We briefly discuss convergence of the effective spectral sequences that we will use. We recall some results of Bachmann–Hopkins [BH20] about motivic Adams operations and of Ananyevskiy–Röndigs–Østvær [ARØ20] about the slices of ko .

The final subsection of Section 2 makes a precise connection between \mathbb{R} -motivic computations and \mathbb{C} -motivic computations. Namely, taking the cofiber of the map ρ changes \mathbb{R} -motivic computations into the analogous \mathbb{C} -motivic computations. This idea originated in [BI20]. This simple observation has surprisingly powerful consequences, especially for the analysis of hidden extensions. It allows us to leverage well-understood \mathbb{C} -motivic information into \mathbb{R} -motivic information.

In Section 2, we have taken some care to eliminate details that we do not use. In other words, Section 2 describes the minimal hypotheses necessary in order to carry out our computations.

Section 3 considers \mathbb{C} -motivic computations, which play two roles in our work. First, they serve as a warmup to the more intricate \mathbb{R} -motivic computations. Second, the comparison between \mathbb{R} -motivic and \mathbb{C} -motivic homotopy is a necessary ingredient for our computations. In this section, we describe the effective spectral sequence for $ko^{\mathbb{C}}$. This material is well-known, since it is the same (up to regrading) as the \mathbb{C} -motivic Adams–Novikov spectral sequence for $ko^{\mathbb{C}}$, which is nearly the same as the classical Adams–Novikov spectral sequence for ko^{top} . We then use the fiber sequence

$$L^{\mathbb{C}} \longrightarrow ko^{\mathbb{C}} \xrightarrow{\psi^3-1} ko^{\mathbb{C}}$$

in order to determine the E_1 -page of the effective spectral sequence for $L^{\mathbb{C}}$.

We next completely analyze the effective spectral sequence for the η -periodicization $L^{\mathbb{C}}[\eta^{-1}]$. The η -periodic spectral sequence is significantly simpler than the unperiodicized spectral sequence. We note the close similarity between the homotopy of $L^{\mathbb{C}}[\eta^{-1}]$ and the computations of Andrew–Miller [AM17].

The η -periodic effective differentials completely determine the unperiodicized effective differentials for $L^{\mathbb{C}}$. Finally, we determine hidden extensions in the effective E_{∞} -page for $L^{\mathbb{C}}$.

Section 3 completely computes the homotopy of $L^{\mathbb{C}}$, but the effective spectral sequence is not necessarily the simplest way of obtaining the computation. Nevertheless, we have chosen this approach because of its relationship to our later \mathbb{R} -motivic computations.

Section 4 analyzes the effective spectral sequence for \mathbb{R} -motivic ko , including all differentials and hidden extensions. The E_1 -page is readily determined from the work of Ananyevskiy–Röndigs–Østvær [ARØ20] on the slices of ko . We draw particular attention to the formula

$$(1.1) \quad (\tau h_1)^2 = \tau^2 \cdot h_1^2 + \rho^2 \cdot v_1^2.$$

This formula has a major impact on the shape of the answers that we obtain. In a sense, our work merely draws algebraic conclusions from Equation (1.1) and η -periodic information. The hidden extensions in the effective E_∞ -page for ko are easily determined by comparison to the \mathbb{C} -motivic case, using the relationship between \mathbb{C} -motivic and \mathbb{R} -motivic homotopy that is described in Section 2.4.

Our computation of the homotopy of \mathbb{R} -motivic ko is not original. See [Kon21] for a C_2 -equivariant analogue of the effective spectral sequence for ko . The \mathbb{R} -motivic computation can be extracted from the C_2 -equivariant computation by dropping the “negative cone” elements. Also, Hill [Hil11] computed the Adams spectral sequence for ko , although the \mathbb{R} -motivic spectrum ko had not yet been constructed at the time.

The next step, undertaken in Section 4.2, is to analyze the effect of ψ^3 on the effective spectral sequence of ko . This follows from a straightforward comparison to the classical case, together with careful bookkeeping. In turn, this leads to a complete understanding of the effective E_1 -page of L , which is described in Section 5.1. Again, this is mostly a matter of careful bookkeeping.

Section 5.2 completely analyzes the effective spectral sequence for η -periodic $L[\eta^{-1}]$. This information is essentially already well-known, either from [GI16] or from Ormsby–Röndigs [OR20], although those references do not specifically mention L .

As in the \mathbb{C} -motivic situation of Section 3, η -periodic information yields everything that we need to know about the unperiodic situation, including all multiplicative relations in the effective E_1 -page for L (see Section 5.3) and all differentials (see Sections 5.4 and 5.5). We again emphasize the significance of Equation (1.1) in carrying out the details. Finally, Section 5.6 studies hidden extensions in the effective E_∞ -page for L . As for ko , these hidden extensions follow by comparison to the \mathbb{C} -motivic case.

1.7. Notation. We use the following notation conventions.

- $v(n)$ is the 2-adic valuation of n , i.e., the largest integer v such that 2^v divides n .
- Except in Section 2, everything is implicitly 2-completed. For example, S is actually the 2-complete \mathbb{R} -motivic sphere spectrum. Similarly, \mathbb{Z} is the 2-adic integers.
- $s_*(X)$ are the slices of a motivic spectrum X .
- $E_r(X)$ is the E_r -page of the effective spectral sequence for a motivic spectrum X .

- We find the effective slice filtration to be slightly inconvenient for our purposes. We prefer to use the “Adams–Novikov filtration”, which equals twice the effective filtration minus the stem.
- Coweight equals the stem minus the motivic weight.
- Elements in $E_r(X)$ are tri-graded. We write $E_r^{s,f,w}(X)$ to denote the part with topological dimension s , Adams–Novikov filtration f , and motivic weight w .
- We use unadorned symbols for \mathbb{R} -motivic spectra. For example, ko is the very effective cover of the \mathbb{R} -motivic Hermitian K -theory spectrum.
- $X^{\mathbb{C}}$ is the \mathbb{C} -motivic extension-of-scalars spectrum of an \mathbb{R} -motivic spectrum X .
- X^{top} is the Betti realization of an \mathbb{R} -motivic spectrum X .
- S is the \mathbb{R} -motivic sphere spectrum.
- KO is the \mathbb{R} -motivic spectrum that represents Hermitian K -theory (also known as KQ).
- ko is the very effective connective cover of KO .
- HA is the \mathbb{R} -motivic Eilenberg–Mac Lane spectrum on the group A .
- ψ^3 is an Adams operation. We use the same symbol in the \mathbb{R} -motivic, \mathbb{C} -motivic, and classical situations.
- L is the fiber of $\mathrm{ko} \xrightarrow{\psi^3-1} \mathrm{ko}$.
- $\Sigma^{s,w}X$ is a (bigraded) suspension of a motivic spectrum X .
- $\pi_{*,*}(X)$ are the bigraded stable homotopy groups of an \mathbb{R} -motivic or \mathbb{C} -motivic spectrum.
- Recall that ε is the motivic homotopy class that is represented by the twist map $S \wedge S \rightarrow S \wedge S$, where S is the motivic sphere spectrum. Let \mathfrak{h} be the element $1 - \varepsilon$, which corresponds to the hyperbolic plane under the isomorphism between $\pi_{0,0}(S)$ and the Grothendieck–Witt ring $GW(\mathbb{R})$ [Mor04].
- The element ρ belongs to the \mathbb{R} -motivic homology of a point. It is the class represented by -1 in the Milnor K -theory of \mathbb{R} . Since ρ survives all of the spectral sequences under consideration, we use the same symbol for the corresponding homotopy class. However, there is a choice of homotopy class represented by ρ because of the presence of elements in higher filtration. There is an inconsistency in the literature about this choice. Following [Bac18], we define ρ such that $\varepsilon = \rho\eta - 1$, or equivalently $2 = \rho\eta + \mathfrak{h}$.

We frequently use names for indecomposables that consist of more than one symbol. For example, Theorem 2.1 discusses the indecomposable element v_1^2 of the effective E_1 -page for $\mathrm{ko}^{\mathbb{C}}$. These longer names are slightly more cumbersome. This is especially the case when we consider products. We will use expressions of the form $x \cdot y$ for clarity.

On the other hand, our names are particularly convenient because they reflect the origins of the elements in terms of the spectral sequences that we use. For example, consider the indecomposable element $2v_1^2$ of the effective E_∞ -page for $\mathrm{ko}^{\mathbb{C}}$,

as discussed in Theorem 3.3 (see also Figure 2). This name reflects the element’s origin in the effective E_1 -page. It also illuminates relations such as

$$2v_1^2 \cdot 2v_1^2 = 4 \cdot v_1^4$$

However, one must be careful about possible error terms in such formulas; see especially Equation (1.1).

2. BACKGROUND

In this section only, we write ko for the integral version of the very effective cover of the Hermitian K -theory spectrum, and we use the usual decorations to indicate localizations and completions of ko . In the rest of the manuscript, ko is assumed to be 2-completed.

2.1. The effective slices of ko . We recall the structure of the effective slices of ko .

Theorem 2.1 ([ARØ20, Theorem 17]). *The slices of ko are*

$$s_*(\mathrm{ko}) = H\mathbb{Z}[h_1, v_1^2]/(2h_1),$$

where v_1^2 and h_1 have degrees $(4, 0, 2)$ and $(1, 1, 1)$ respectively.

We explain the expression in Theorem 2.1. Each monomial of degree (s, f, w) contributes a summand of $\Sigma^{s,w}HA$ in the $\left(\frac{s+f}{2}\right)$ th slice. Here HA is the motivic Eilenberg–Mac Lane spectrum associated to A . The abelian group A is \mathbb{F}_2 when the monomial is 2-torsion, and is \mathbb{Z} when the monomial is torsion free. We list the first three slices as examples:

$$\begin{aligned} s_0(\mathrm{ko}) &= H\mathbb{Z}\{1\}, \\ s_1(\mathrm{ko}) &= \Sigma^{1,1}H\mathbb{F}_2\{h_1\}, \\ s_2(\mathrm{ko}) &= \Sigma^{2,2}H\mathbb{F}_2\{h_1^2\} \vee \Sigma^{4,2}H\mathbb{Z}\{v_1^2\}. \end{aligned}$$

Beware that the multiplicative structure of $s_*(\mathrm{ko})$ is not completely captured by the notation in Theorem 2.1. The essential multiplicative relation is Equation (1.1), which follows immediately from the general formulas in [ARØ20].

Remark 2.2. The calculation of the slices of the motivic sphere spectrum, due to Röndigs, Spitzweck, and Østvær [RSØ19], is commonly expressed at the prime 2 as

$$s_*(S) = H\mathbb{Z} \otimes \mathrm{Ext}_{BP_*BP}^{*,*}(BP_*, BP_*).$$

Analogously, Theorem 2.1 says that

$$s_*(\mathrm{ko}) = H\mathbb{Z} \otimes \mathrm{Ext}_{BP_*BP}^{*,*}(BP_*, BP_*(\mathrm{ko}^{\mathrm{top}})).$$

However, we do not know of a general theorem relating the slices of a motivic spectrum with the Adams–Novikov E_2 -page for its topological counterpart.

2.2. The Adams operation ψ^3 and the spectrum L . Bachmann and Hopkins [BH20] constructed a motivic analogue of the classical Adams operation ψ^3 . We summarize the results that we need.

Theorem 2.3 ([BH20]). *There is a unital ring map $\psi^3 : \mathbf{ko} \left[\frac{1}{3} \right] \rightarrow \mathbf{ko} \left[\frac{1}{3} \right]$ whose Betti realization is the classical Adams operation ψ^3 .*

Proof. There is a unital ring map $\psi^3 : \mathbf{KO} \left[\frac{1}{3} \right] \rightarrow \mathbf{KO} \left[\frac{1}{3} \right]$ [BH20, Theorem 3.1], which is an E_∞ -map. Its Betti realization is also an E_∞ -map whose action on the classical Bott element is multiplication by 81. These properties uniquely characterize the classical Adams operation.

Now apply very effective covers, and the result about \mathbf{ko} follows formally. \square

The original result is more general in more than one sense. First, it works over general base schemes in which 2 is invertible, while we only use the construction over \mathbb{R} . Second, its values are computed more precisely than just compatibility with the classical values.

Corollary 2.4.

- (1) $\psi^3 : \pi_{*,*}(\mathbf{ko}_2^\wedge) \rightarrow \pi_{*,*}(\mathbf{ko}_2^\wedge)$ is a ring map.
- (2) If x is in the image of the unit map $\pi_{*,*}(S_2^\wedge) \rightarrow \pi_{*,*}(\mathbf{ko}_2^\wedge)$, then $\psi^3(x) = x$.
- (3) There is a commutative diagram

$$\begin{array}{ccc} \pi_{*,*}(\mathbf{ko}_2^\wedge) & \xrightarrow{\psi^3} & \pi_{*,*}(\mathbf{ko}_2^\wedge) \\ \downarrow & & \downarrow \\ \pi_*(\mathbf{ko}^{\text{top}})_2^\wedge & \xrightarrow{\psi^3} & \pi_*(\mathbf{ko}^{\text{top}})_2^\wedge, \end{array}$$

where the vertical maps are Betti realization homomorphisms.

Proof. These are computational consequences of Theorem 2.3. Part (1) follows from the fact that ψ^3 is a ring map. Part (2) follows from the fact that ψ^3 is unital. Part (3) follows from the fact that the Betti realization of the motivic Adams operation is the classical Adams operation. \square

Remark 2.5. Corollary 2.4 can also be stated in a localized sense rather than completed sense, but we will not need that.

Definition 2.6. Let L be the fiber of the map $\mathbf{ko} \left[\frac{1}{3} \right] \xrightarrow{\psi^3-1} \mathbf{ko} \left[\frac{1}{3} \right]$.

Note that our definition of L is already localized; we do not consider an integral version. Except for this section, L is assumed to be 2-completed.

The most important point for us is that there is a fiber sequence

$$L_2^\wedge \longrightarrow \mathbf{ko}_2^\wedge \xrightarrow{\psi^3-1} \mathbf{ko}_2^\wedge$$

of completed spectra since completion preserves fiber sequences.

2.3. Convergence of the effective spectral sequence. The *effective spectral sequence* for a motivic spectrum X denotes the spectral sequence associated to

the effective slice filtration of X . We refer to [Lev13, RSØ19] for details on the construction and properties of this spectral sequence.

The effective slice filtration [Voe02] has truncations $f^q(X)$ and quotients (i.e., slices) $s_q(X)$. The E_1 -page of the effective spectral sequence is $\pi_{*,*}(s_*(X))$. In good cases, it converges to the homotopy groups of a completion of X . We also use the very effective slice filtration [SØ12], but only to define ko .

The slice functors do not necessarily commute with completions, i.e., $s_*(X)_2^\wedge$ and $s_*(X_2^\wedge)$ are not always equivalent. Consequently, we must carefully define the spectral sequences that we use to study completed spectra. On the other hand, the effective slices do interact nicely with localizations [Spi08, Corollary 4.6].

Theorem 2.7. *There are strongly convergent spectral sequences*

$$E_1^{s,f,w}(\mathrm{ko}) = \pi_{s,w} \left(s_{\frac{s+f}{2}}(\mathrm{ko})_2^\wedge \right) \implies \pi_{s,w}(\mathrm{ko}_2^\wedge)$$

and

$$E_1^{s,f,w}(L) = \pi_{s,w} \left(s_{\frac{s+f}{2}}(L)_2^\wedge \right) \implies \pi_{s,w}(L_2^\wedge)$$

with differentials $d_r : E_r^{s,f,w} \rightarrow E_r^{s-1,f+2r-1,w}$.

We remind the reader that our grading of the effective spectral sequence is different than the standard grading in the literature. Briefly, s represents the topological stem, f represents the Adams–Novikov filtration (not the effective filtration), and w represents the motivic weight. See Section 1.7 for more discussion.

Proof. We discuss the spectral sequence for ko in detail; most of the argument for L is the same.

Consider the effective slice tower

$$f^0(\mathrm{ko}) \leftarrow f^1(\mathrm{ko}) \leftarrow f^2(\mathrm{ko}) \leftarrow \cdots$$

Now take the 2-completion of this tower to obtain

$$f^0(\mathrm{ko})_2^\wedge \leftarrow f^1(\mathrm{ko})_2^\wedge \leftarrow f^2(\mathrm{ko})_2^\wedge \leftarrow \cdots$$

The resulting layers are the same as $s_*(\mathrm{ko})_2^\wedge$ since completion respects cofiber sequences. Beware that this is not necessarily the same as the slice tower of the completion ko_2^\wedge , since slices do not interact nicely with completions. The associated spectral sequence of this tower is the one described in the statement of the theorem.

It remains to determine the target of the completed spectral sequence. The limit of the uncompleted slice tower of ko is equivalent to its η -completion [RSØ19], [ARØ20], i.e.,

$$\mathrm{holim} f^n(\mathrm{ko}) \simeq \mathrm{ko}_\eta^\wedge.$$

Completion respects limits, so the limit $\mathrm{holim}(f^n(\mathrm{ko})_2^\wedge)$ of the completed slice tower is equivalent to $(\mathrm{ko}_\eta^\wedge)_2^\wedge$, which is equivalent to ko_2^\wedge by [HKO11, Theorem 1]. Consequently, the completed effective spectral sequence of ko converges to the homotopy of ko_2^\wedge , as desired.

Strong convergence follows from [Boa99, Theorem 7.1], which has a technical hypothesis involving derived E_∞ -pages. For ko , this technical hypothesis follows directly from the computations of Section 4. For L , the technical hypothesis follows directly from the computations in Sections 5.4 and 5.5. \square

Remark 2.8. By construction, we have a fiber sequence

$$s_*(L)_2^\wedge \longrightarrow s_*(\mathbf{ko})_2^\wedge \xrightarrow{\psi^3-1} s_*(\mathbf{ko})_2^\wedge,$$

which yields a long exact sequence

$$\cdots \longrightarrow E_1^{s,f,w}(L) \longrightarrow E_1^{s,f,w}(\mathbf{ko}) \xrightarrow{\psi^3-1} E_1^{s,f,w}(\mathbf{ko}) \longrightarrow \cdots.$$

This long exact sequence will be our main tool for computing $E_1(L)$ in Section 5.1.

2.4. Comparison between \mathbb{R} -motivic and \mathbb{C} -motivic homotopy. Extension of scalars induces a functor $(-)^{\mathbb{C}}$ from \mathbb{R} -motivic stable homotopy theory to \mathbb{C} -motivic stable homotopy theory. Following [BI20, Section 3], we recall its computational interpretation. These results will play a central role later in Section 5.6 when we consider hidden extensions.

The homotopy element ρ maps to zero under extension of scalars. Therefore, extension of scalars induces a natural homomorphism

$$\pi_{*,*}(X/\rho) \rightarrow \pi_{*,*}(X^{\mathbb{C}})$$

for any \mathbb{R} -motivic spectrum X .

Proposition 2.9. *The maps*

$$\pi_{*,*}(\mathbf{ko}/\rho) \rightarrow \pi_{*,*}(\mathbf{ko}^{\mathbb{C}})$$

and

$$\pi_{*,*}(L/\rho) \rightarrow \pi_{*,*}(L^{\mathbb{C}})$$

are isomorphisms.

Proof. The argument for the first isomorphism is essentially identical to the argument in [BI20, Section 3]. We need that the Adams E_2 -page for \mathbf{ko} is computed by the cobar complex associated to the subalgebra $A(1)$ of the motivic Steenrod algebra, and multiplication by ρ is injective on this cobar complex.

For the second isomorphism, consider the diagram

$$\begin{array}{ccccccc} \cdots & \longrightarrow & \pi_{*,*}(L/\rho) & \longrightarrow & \pi_{*,*}(\mathbf{ko}/\rho) & \longrightarrow & \pi_{*,*}(\mathbf{ko}/\rho) \longrightarrow \cdots \\ & & \downarrow & & \downarrow & & \downarrow \\ \cdots & \longrightarrow & \pi_{*,*}(L^{\mathbb{C}}) & \longrightarrow & \pi_{*,*}(\mathbf{ko}^{\mathbb{C}}) & \longrightarrow & \pi_{*,*}(\mathbf{ko}^{\mathbb{C}}) \longrightarrow \cdots \end{array}$$

The vertical maps are induced by extension of scalars. The horizontal maps arise from the fiber sequence

$$L \longrightarrow \mathbf{ko} \xrightarrow{\psi^3-1} \mathbf{ko},$$

so the rows are exact. We already know that the second and third vertical arrows are isomorphisms, so the first vertical arrow is also an isomorphism by the Five Lemma. \square

3. \mathbb{C} -MOTIVIC COMPUTATIONS

In this section, we carry out a preliminary computation of the effective spectral sequences for $\mathbf{ko}^{\mathbb{C}}$ and $L^{\mathbb{C}}$. We also consider the η -periodic spectral sequences. We

are primarily interested in \mathbb{R} -motivic computations, but we will need to compare our \mathbb{R} -motivic computations to their \mathbb{C} -motivic counterparts.

3.1. The effective spectral sequence for $\mathbf{ko}^{\mathbb{C}}$. We review the effective spectral sequence for $\mathbf{ko}^{\mathbb{C}}$.

Proposition 3.1. *The effective spectral sequence for $\mathbf{ko}^{\mathbb{C}}$ takes the form*

$$E_1(\mathbf{ko}^{\mathbb{C}}) = \mathbb{Z}[\tau, h_1, v_1^2]/2h_1.$$

Proof. This follows from Theorem 2.1 by taking stable homotopy groups. There are no possible error terms to complicate the multiplicative structure. \square

Table 1 lists the generators of $E_1(\mathbf{ko}^{\mathbb{C}})$. Figure 1 depicts $E_1(\mathbf{ko}^{\mathbb{C}})$ in graphical form.

Table 1: Multiplicative generators for $E_1(\mathbf{ko}^{\mathbb{C}})$

coweight	(s, f, w)	x	$d_1(x)$	$\psi^3(x)$
0	(1, 1, 1)	h_1		h_1
1	(0, 0, -1)	τ		τ
2	(4, 0, 2)	v_1^2	τh_1^3	$9v_1^2$

Proposition 3.2. *Table 1 gives the values of the effective d_1 differential on the multiplicative generators of $E_1(\mathbf{ko}^{\mathbb{C}})$.*

Proof. The \mathbb{C} -motivic effective spectral sequence is identical to the \mathbb{C} -motivic Adams–Novikov spectral sequence up to reindexing. This claim does not appear to be cleanly stated in the literature, but it is a computational consequence of the weight 0 result of [Lev15, Theorem 1]. Alternatively, there is only one pattern of effective differentials that computes the motivic stable homotopy groups of $\mathbf{ko}^{\mathbb{C}}$, which were previously described using the \mathbb{C} -motivic Adams spectral sequence [IS11]. \square

Theorem 3.3. *The E_∞ -page of the effective spectral sequence for $\mathbf{ko}^{\mathbb{C}}$ takes the form*

$$E_\infty(\mathbf{ko}^{\mathbb{C}}) = \frac{\mathbb{Z}[\tau, h_1, 2v_1^2, v_1^4]}{2h_1, \tau h_1^3, (2v_1^2)^2 = 4 \cdot v_1^4}.$$

Proof. For degree reasons, there can be no higher differentials in the effective spectral sequence for $\mathbf{ko}^{\mathbb{C}}$. \square

Table 2 lists the multiplicative generators of $E_\infty(\mathbf{ko}^{\mathbb{C}})$. Figure 2 depicts $E_\infty(\mathbf{ko}^{\mathbb{C}})$ in graphical form.

Table 2: Multiplicative generators for $E_\infty(\mathbf{ko}^{\mathbb{C}})$

coweight	(s, f, w)	x	$\psi^3(x)$
0	(1, 1, 1)	h_1	h_1
1	(0, 0, -1)	τ	τ
2	(4, 0, 2)	$2v_1^2$	$9 \cdot 2v_1^2$
4	(8, 0, 4)	v_1^4	$81v_1^4$

Remark 3.4. There are no possible hidden extensions in $E_\infty(\mathbf{ko}^{\mathbb{C}})$ for degree reasons. Therefore, Theorem 3.3 describes $\pi_{*,*}(\mathbf{ko}^{\mathbb{C}})$ as a ring.

3.2. The effective E_1 -page for $L^{\mathbb{C}}$. Our next goal is to describe the effective E_1 -page $E_1(L^{\mathbb{C}})$. First we must study the values of ψ^3 on $\mathbf{ko}^{\mathbb{C}}$.

Lemma 3.5. *The map $E_\infty(\mathbf{ko}^{\mathbb{C}}) \rightarrow E_\infty(\mathbf{ko}^{\mathbb{C}})$ induced by ψ^3 on effective E_∞ -pages takes the values shown in Table 2.*

Proof. All values follow immediately by comparison along Betti realization to the values of classical ψ^3 . \square

Lemma 3.6. *The map $E_1(\mathbf{ko}^{\mathbb{C}}) \rightarrow E_1(\mathbf{ko}^{\mathbb{C}})$ induced by ψ^3 on effective E_1 -pages takes the values shown in Table 1.*

Proof. The values of ψ^3 on $E_1(\mathbf{ko}^{\mathbb{C}})$ are compatible with the values of ψ^3 on $E_\infty(\mathbf{ko}^{\mathbb{C}})$, as shown in Table 2 (see also Lemma 3.5). This immediately yields all values. \square

In order to describe $E_1(L^{\mathbb{C}})$, we need some elementary number theory.

Definition 3.7. Let $v(n)$ be the 2-adic valuation of n , i.e., the exponent of the largest power of 2 that divides n .

Lemma 3.8.

$$v(3^n - 1) = \begin{cases} 1 & \text{if } v(n) = 0 \\ 2 + v(n) & \text{if } v(n) > 0 \end{cases}$$

Proof. Let $n = 2^a \cdot b$, where b is an odd number, so $v(n) = a$. Then

$$3^n - 1 = \left(1 + 3^{2^a} + (3^{2^a})^2 + \cdots + (3^{2^a})^{b-1}\right) (3 - 1) \prod_{i=0}^{a-1} (1 + 3^{2^i}).$$

The first factor is odd, so it does not contribute to the 2-adic valuation. The factor $(1 + 3^{2^i})$ has valuation 1 if $i > 0$, and it has valuation 2 if $i = 0$. \square

Proposition 3.9. *The chart in Figure 3 depicts the effective E_1 -page of $L^{\mathbb{C}}$.*

Proof. The long exact sequence

$$\cdots \longrightarrow E_1(L^{\mathbb{C}}) \longrightarrow E_1(\mathrm{ko}^{\mathbb{C}}) \xrightarrow{\psi^{3-1}} E_1(\mathrm{ko}^{\mathbb{C}}) \longrightarrow \cdots$$

induces a short exact sequence

$$0 \longrightarrow \Sigma^{-1}C \longrightarrow E_1(L^{\mathbb{C}}) \longrightarrow K \longrightarrow 0,$$

where C and K are the cokernel and kernel of $E_1(\mathrm{ko}^{\mathbb{C}}) \xrightarrow{\psi^{3-1}} E_1(\mathrm{ko}^{\mathbb{C}})$ respectively. The cokernel and kernel can be computed directly from the information given in Table 1 (see also Lemma 3.6).

The kernel is additively generated by all multiples of h_1 in $E_1(\mathrm{ko}^{\mathbb{C}})$, together with the elements τ^k for $k \geq 0$.

The cokernel C is nearly the same as $E_1(\mathrm{ko}^{\mathbb{C}})$ itself. We must impose the relations $(3^{2k} - 1)v_1^{2k} = 0$ for all $k > 0$. Lemma 3.8 says that $3^{2k} - 1$ equals $2^{v(2k)+2} \cdot u$, where u is an odd number, i.e., a unit in our 2-adic context. Therefore, the relation $(3^{2k} - 1)v_1^{2k} = 0$ is equivalent to the relation $2^{v(2k)+2}v_1^{2k} = 0$. \square

Table 3 lists some elements of the effective E_1 -page of $L^{\mathbb{C}}$. In fact, these elements are multiplicative generators for $E_1(L^{\mathbb{C}})$. By inspection, all elements of $E_1(L^{\mathbb{C}})$ are of the form $\tau^a h_1^b x$, for some x in the table.

We use the same notation for elements of $E_1(L^{\mathbb{C}})$ and their images in $E_1(\mathrm{ko}^{\mathbb{C}})$. On the other hand, we define the elements ιx of $E_1(L^{\mathbb{C}})$ by the property that they are the image of x under the map $\iota : \Sigma^{-1}E_1(\mathrm{ko}) \rightarrow E_1(L)$. For example, the element 1 of $E_1(\mathrm{ko})$ maps to ι .

Table 3: Multiplicative generators for $E_1(L^{\mathbb{C}})$: $k \geq 0$

coweight	(s, f, w)	generator
1	$(0, 0, -1)$	τ
$2k$	$(4k + 1, 1, 2k + 1)$	$h_1 v_1^{2k}$
$2k - 1$	$(4k - 1, 1, 2k)$	ιv_1^{2k}

Remark 3.10. Our choice of notation for elements of $E_1(L^{\mathbb{C}})$ is helpful for the particular analysis at hand. The generators of $E_1(L^{\mathbb{C}})$ also have traditional names from the perspective of the Adams–Novikov spectral sequence. Namely, $h_1 v_1^{2k}$ and ιv_1^{2k} correspond to α_{2k+1} and $\alpha_{2k/v(8k)}$ respectively. However, the α -family perspective is not so helpful for us.

3.3. The effective spectral sequence of $L^{\mathbb{C}}[\eta^{-1}]$. Next, we describe the effective spectral sequence of $L^{\mathbb{C}}[\eta^{-1}]$.

In the η -periodic context, the element h_1 is a unit. Therefore, powers of h_1 are inconsequential for computational purposes. Consequently, we have removed these powers from all η -periodic formulas. The appropriate powers of h_1 can be easily

reconstructed from the degrees of elements (although this reconstruction is typically not necessary).

Proposition 3.11. *The effective E_1 -page for $L^{\mathbb{C}}[\eta^{-1}]$ is given by*

$$E_1(L^{\mathbb{C}}[\eta^{-1}]) = \mathbb{F}_2[h_1^{\pm 1}, \tau, v_1^2, \iota]/\iota^2.$$

Proof. The functors s_* commute with homotopy colimits [Spi08, Corollary 4.6]. Therefore, we can just invert h_1 in $E_1(\mathrm{ko}^{\mathbb{C}})$ to obtain

$$E_1(\mathrm{ko}^{\mathbb{C}}[\eta^{-1}]) = \mathbb{F}_2[h_1^{\pm 1}, \tau, v_1^2].$$

See Proposition 3.1 (and Figure 1) for the description of $E_1(\mathrm{ko}^{\mathbb{C}})$.

The map $E_1(\mathrm{ko}^{\mathbb{C}}[\eta^{-1}]) \xrightarrow{\psi^3-1} E_1(\mathrm{ko}^{\mathbb{C}}[\eta^{-1}])$ is trivial because $(\psi^3 - 1)(h_1) = 0$, as shown in Table 1 (see also Lemma 3.6). Therefore, the long exact sequence

$$\cdots \longrightarrow E_1(L^{\mathbb{C}}[\eta^{-1}]) \longrightarrow E_1(\mathrm{ko}^{\mathbb{C}}[\eta^{-1}]) \xrightarrow{\psi^3-1} E_1(\mathrm{ko}^{\mathbb{C}}[\eta^{-1}]) \longrightarrow \cdots$$

implies that $E_1(L^{\mathbb{C}}[\eta^{-1}])$ splits as

$$E_1(\mathrm{ko}^{\mathbb{C}}[\eta^{-1}]) \oplus \Sigma^{-1}E_1(\mathrm{ko}^{\mathbb{C}}[\eta^{-1}]).$$

This establishes the additive structure of $E_1(L[\eta^{-1}])$, as well as most of the multiplicative structure.

The relation $\iota^2 = 0$ is immediate because there are no possible non-zero values for ι^2 . \square

Proposition 3.12. *In the effective spectral sequence for $L^{\mathbb{C}}[\eta^{-1}]$, we have $d_1(v_1^2) = \tau$. The effective differentials are zero on all other multiplicative generators on all pages.*

Proof. The value of $d_1(v_1^2)$ in $E_1(L^{\mathbb{C}}[\eta^{-1}])$ follows by comparison of effective spectral sequences along the maps $L^{\mathbb{C}} \rightarrow L^{\mathbb{C}}[\eta^{-1}]$ and $L^{\mathbb{C}} \rightarrow \mathrm{ko}^{\mathbb{C}}$. Table 1 (see also Proposition 3.2) gives the value of $d_1(v_1^2)$ in $E_1(\mathrm{ko}^{\mathbb{C}})$. \square

Remark 3.13. The effective spectral sequence for $L^{\mathbb{C}}[\eta^{-1}]$ is very close to the effective spectral sequence for the η -periodic sphere $S^{\mathbb{C}}[\eta^{-1}]$. The effective spectral sequence for $S^{\mathbb{C}}[\eta^{-1}]$ is the same (up to reindexing) as the motivic Adams–Novikov spectral sequence for $S^{\mathbb{C}}[\eta^{-1}]$. This motivic Adams–Novikov spectral sequence is analyzed in [AM17]. The element ι is not present in $E_1(S^{\mathbb{C}}[\eta^{-1}])$, but its multiples $\iota(v_1^2)^k$ are present.

3.4. Effective differentials for $L^{\mathbb{C}}$.

Proposition 3.14. *Table 4 gives the values of the effective d_1 differentials on the multiplicative generators of $E_1(L^{\mathbb{C}})$. There are no higher differentials in the effective spectral sequence for $L^{\mathbb{C}}$.*

Proof. All of these differentials follow immediately from the effective d_1 differentials for $L^{\mathbb{C}}[\eta^{-1}]$, which are determined by Proposition 3.12.

For degree reasons, there are no possible higher differentials. \square

Table 4: Effective d_1 differentials for $L^{\mathbb{C}}$: $k \geq 0$

coweight	(s, f, w)	x	$d_1(x)$
1	$(0, 0, -1)$	τ	
$4k$	$(8k + 1, 1, 4k + 1)$	$h_1 v_1^{4k}$	
$4k + 2$	$(8k + 5, 1, 4k + 3)$	$h_1 v_1^{4k+2}$	$\tau h_1^3 \cdot h_1 v_1^{4k}$
$4k - 1$	$(8k - 1, 1, 4k)$	ιv_1^{4k}	
$4k + 1$	$(8k + 3, 1, 4k + 2)$	ιv_1^{4k+2}	$\tau h_1^3 \cdot \iota v_1^{4k}$

Theorem 3.15. *The E_∞ -page of the effective spectral sequence for $L^{\mathbb{C}}$ is depicted in Figure 4.*

Proof. Because there are no higher effective differentials for $L^{\mathbb{C}}$, we obtain the effective E_∞ -page immediately from the effective d_1 differentials in Table 4 (see also Proposition 3.14). \square

3.5. Hidden extensions in $E_\infty(L^{\mathbb{C}})$.

Proposition 3.16. *In the effective spectral sequence for $L^{\mathbb{C}}$, there are hidden \mathfrak{h} extensions from ιv_1^{4k+2} to $\tau h_1^2 \cdot h_1 v_1^{4k}$ for all $k \geq 0$.*

Proof. Recall that $\tau\eta^2 = \langle \mathfrak{h}, \eta, \mathfrak{h} \rangle$ in the homotopy of the \mathbb{C} -motivic sphere [Isa19, Table 7.23]. If α is a homotopy element of $L^{\mathbb{C}}$ such that $\mathfrak{h}\alpha$ is zero, then

$$\alpha \cdot \tau\eta^2 = \alpha \langle \mathfrak{h}, \eta, \mathfrak{h} \rangle = \langle \alpha, \mathfrak{h}, \eta \rangle \mathfrak{h}.$$

In particular, let α be detected by $h_1 v_1^{4k}$. Then $\tau h_1^2 \cdot h_1 v_1^{4k}$ detects a homotopy element that is divisible by \mathfrak{h} , so $\tau h_1^2 \cdot h_1 v_1^{4k}$ must be the target of a hidden \mathfrak{h} extension. There is only one possible source for this extension. \square

4. THE EFFECTIVE SPECTRAL SEQUENCE FOR \mathfrak{ko}

We now study the effective spectral sequence for \mathbb{R} -motivic \mathfrak{ko} .

Proposition 4.1. *The effective spectral sequence for \mathfrak{ko} takes the form*

$$E_1(\mathfrak{ko}) = \frac{\mathbb{Z}[\rho, \tau^2, h_1, \tau h_1, v_1^2]}{2\rho, 2h_1, 2 \cdot \tau h_1, (\tau h_1)^2 = \tau^2 \cdot h_1^2 + \rho^2 \cdot v_1^2}$$

Proof. The additive structure follows from Theorem 2.1 by taking stable homotopy groups. We need that the homotopy groups of \mathbb{R} -motivic $H\mathbb{Z}$ are

$$H\mathbb{Z}_{*,*} = \mathbb{Z}[\tau^2, \rho]/2\rho,$$

and the homotopy groups of \mathbb{R} -motivic $H\mathbb{F}_2$ are

$$(H\mathbb{F}_2)_{*,*} = \mathbb{F}_2[\tau, \rho].$$

The multiplicative structure is mostly also immediate from Theorem 2.1. As explained in [Kon21], our formula for $(\tau h_1)^2$ is equivalent to the formula $\eta^2 \xrightarrow{\delta} \sqrt{\alpha}$ given in [ARØ20, p. 1029]. \square

Table 5 lists the generators of $E_1(\mathbf{ko})$. Figure 5 depicts $E_1(\mathbf{ko})$ in graphical form.

Table 5: Multiplicative generators for $E_1(\mathbf{ko})$

coweight	(s, f, w)	x	$d_1(x)$	$\psi^3(x)$	image in $E_1(\mathbf{ko}[\eta^{-1}])$
0	$(-1, 1, -1)$	ρ		ρ	ρ
0	$(1, 1, 1)$	h_1		h_1	1
1	$(1, 1, 0)$	τh_1		τh_1	τ
2	$(0, 0, -2)$	τ^2	$\rho^2 \cdot \tau h_1$	τ^2	$\tau^2 + \rho^2 \cdot v_1^2$
2	$(4, 0, 2)$	v_1^2	$\tau h_1 \cdot h_1^2$	$9v_1^2$	v_1^2

Proposition 4.2. *Table 5 gives the values of the effective d_1 differential on the multiplicative generators of $E_1(\mathbf{ko})$.*

Proof. The value of $d_1(\tau^2)$ follows from [ARØ20, Theorem 20] and \mathbb{R} -motivic Steenrod algebra actions. Then the value of $d_1(v_1^2)$ follows from Equation (1.1).

Alternatively, there is only one pattern of effective differentials that computes the motivic stable homotopy groups of \mathbf{ko} , which were previously computed with the \mathbb{R} -motivic Adams spectral sequence [Hil11]. \square

The entire d_1 differential in the effective spectral sequence for \mathbf{ko} can easily be deduced from Proposition 4.2 and the Leibniz rule.

Theorem 4.3. *The E_∞ -page of the effective spectral sequence for \mathbf{ko} is depicted in Figures 6, 7, and 8.*

Proof. The Leibniz rule, together with the values in Table 5 (see also Proposition 4.2), completely determines the effective d_1 differential on $E_1(\mathbf{ko})$. The E_2 -page can then be determined directly. However, the computation is not entirely straightforward. Of particular note is the differential

$$d_1(\tau^2 \cdot \tau h_1 \cdot v_1^2) = \tau^4 \cdot h_1^4 + \rho^4 \cdot v_1^4,$$

which yields the relation

$$(4.1) \quad \tau^4 \cdot h_1^4 = \rho^4 \cdot v_1^4$$

in $E_2(\mathbf{ko})$.

For degree reasons, there can be no higher differentials in the effective spectral sequence for \mathbf{ko} . \square

For legibility, Figures 6, 7, and 8 display $E_\infty(\mathfrak{ko})$ in three different charts separated by coweight modulo 4. There is no chart for coweights $3 \bmod 4$ because $E_\infty(\mathfrak{ko})$ is zero in those coweights.

Figure 9 illustrates part of the analysis of the d_1 differentials and the determination of $E_2(\mathfrak{ko})$; it is meant to be representative, not thorough. The chart shows some of the elements in coweights 1 and 2 mod 4, together with the d_1 differentials that relate these elements. In this chart, one can see that $\tau^2 \cdot h_1^2 + \rho^2 \cdot v_1^2$ survives to $E_2(\mathfrak{ko})$. This element survives to $E_\infty(\mathfrak{ko})$. It is labelled $(\tau h_1)^2$ in Figure 8, in accordance with Equation (1.1).

Remark 4.4. There is an alternative, slightly more structured, method for obtaining $E_\infty(\mathfrak{ko})$. One can filter $E_1(\mathfrak{ko})$ by powers of τh_1 and obtain a spectral sequence that converges to $E_2(\mathfrak{ko})$. In this spectral sequence, we have the relation $\tau^2 \cdot h_1^2 = \rho^2 \cdot v_1^2$. There are differentials $d_1(\tau^2) = \rho^2 \cdot \tau h_1$ and $d_1(v_1^2) = h_1^2 \cdot \tau h_1$. Then there is a higher differential $d_3(\tau^2 \cdot v_1^2) = (\tau h_1)^3$. None of this is essential to our study, but the interested reader may wish to carry out the details.

Table 6 lists the multiplicative generators of $E_\infty(\mathfrak{ko})$. It is possible to give a complete list of relations. However, the long list is not so helpful for understanding the structure of $E_\infty(\mathfrak{ko})$. The charts in Figures 6, 7, and 8 are more useful for this purpose.

Table 6: Multiplicative generators for $E_\infty(\mathfrak{ko})$

coweight	(s, f, w)	x	$\psi^3(x)$
0	$(-1, 1, -1)$	ρ	ρ
0	$(1, 1, 1)$	h_1	h_1
1	$(1, 1, 0)$	τh_1	τh_1
2	$(0, 0, -2)$	$2\tau^2$	$2\tau^2$
2	$(4, 0, 2)$	$2v_1^2$	$9 \cdot 2v_1^2$
4	$(0, 0, -4)$	τ^4	τ^4
4	$(4, 0, 0)$	$2\tau^2 v_1^2$	$9 \cdot 2\tau^2 v_1^2$
4	$(8, 0, 4)$	v_1^4	$81v_1^4$

Proposition 4.5. *Table 7 lists some hidden extensions by ρ , \mathfrak{h} , and η in the effective spectral sequence for \mathfrak{ko} . All other hidden extensions by ρ , \mathfrak{h} , and η are v_1^4 -multiples and τ^4 -multiples of these.*

Proof. Recall from Proposition 2.9 that the homotopy of \mathfrak{ko}/ρ is isomorphic to the homotopy of $\mathfrak{ko}^{\mathbb{C}}$. Therefore, we completely understand the homotopy of \mathfrak{ko}/ρ from Theorem 3.3 and Figure 2.

The hidden ρ extensions follow from inspection of the long exact sequence associated to the cofiber sequence

$$\Sigma^{-1,-1}\mathbf{ko} \xrightarrow{\rho} \mathbf{ko} \rightarrow \mathbf{ko}/\rho.$$

The map $\mathbf{ko} \rightarrow \mathbf{ko}/\rho$ takes the elements $\tau^4 \cdot h_1^3$ and $(\tau h_1)^2 h_1$ to zero because there are no possible targets in the homotopy of \mathbf{ko}/ρ . Therefore, those two elements must receive hidden ρ extensions, and there is only one possibility in both cases.

The relation $\tau^4 \cdot h_1^4 = \rho^4 \cdot v_1^4$ (see Equation (4.1)) then implies that $2\tau^2 v_1^2$ also supports an h_1 extension.

The map $\mathbf{ko}/\rho \rightarrow \Sigma^{0,-1}\mathbf{ko}$ takes τ^3 and $\tau^3 h_1$ to $2\tau^2$ and $\rho(\tau h_1)^2$ respectively. There is an h_1 extension connecting τ^3 and $\tau^3 h_1$ in \mathbf{ko}/ρ , so there must be a hidden η extension from $2\tau^2$ to $\rho(\tau h_1)^2$.

The hidden h extension on τh_1 follows from the analogous hidden extension in the homotopy groups of the \mathbb{R} -motivic sphere [DI17] [BI20], using the unit map $S \rightarrow \mathbf{ko}$. Alternatively, this hidden extension is computed in [Hil11, Proposition 4.3] in the context of the \mathbb{R} -motivic Adams spectral sequence for \mathbf{ko} .

Finally, multiply by τh_1 to obtain the hidden h extension on $(\tau h_1)^2$.

For degree reasons, there are no other possible hidden extensions to consider. \square

Table 7: Hidden extensions in $E_\infty(\mathbf{ko})$

coweight	source	type	target	(s, f, w)
2	$2v_1^2$	ρ	$(\tau h_1)^2 h_1$	$(3, 3, 1)$
4	$2\tau^2 v_1^2$	ρ	$\tau^4 \cdot h_1^3$	$(3, 3, -1)$
4	$2\tau^2 v_1^2$	η	$\rho^3 \cdot v_1^4$	$(5, 3, 1)$
2	$2\tau^2$	η	$\rho(\tau h_1)^2$	$(1, 3, -1)$
1	τh_1	h	$\rho \cdot \tau h_1 \cdot h_1$	$(1, 3, 0)$
2	$(\tau h_1)^2$	h	$\rho(\tau h_1)^2 h_1$	$(2, 4, 0)$

Remark 4.6. We have completely analyzed the E_∞ -page of the effective spectral sequence for \mathbf{ko} , but this is not quite the same as completely describing the homotopy of \mathbf{ko} . In particular, one must choose an element of $\pi_{*,*}\mathbf{ko}$ that is represented by each multiplicative generator of $E_\infty(\mathbf{ko})$ (see Table 6). In some cases, there is more than one choice because of the presence of elements in higher filtration in the E_∞ -page. The choices of ρ , h_1 , τh_1 , and τ^4 can be made arbitrarily; the ring structure is unaffected by these choices. The elements $2\tau^2$ and $2v_1^2$ are already well-defined because there are no elements in higher filtration. Finally, the choices of $2\tau^2 v_1^2$ and v_1^4 can then be uniquely specified by the relations $\rho \cdot 2\tau^2 v_1^2 = \tau^4 \cdot h_1^3$ and $\rho^4 \cdot v_1^4 = \tau^4 \cdot h_1^4$.

4.1. η -periodic \mathbf{ko} . Later we will need some information about the η -periodic spectrum $\mathbf{ko}[\eta^{-1}]$. As in Section 3.3, powers of h_1 are inconsequential for computational

purposes in the η -periodic context. Consequently, we have removed these powers from all η -periodic formulas.

Proposition 4.7. *The effective E_1 -page for \mathbf{ko} is given by*

$$E_1(\mathbf{ko}[\eta^{-1}]) = \mathbb{F}_2[h_1^{\pm 1}, \tau, \rho, v_1^2].$$

Moreover, the periodicization map $\mathbf{ko} \rightarrow \mathbf{ko}[\eta^{-1}]$ induces the map on effective E_1 -pages whose values are given in Table 5.

The first part of Proposition 4.7 was first proved in [ARØ20, Theorem 19], although the notation is different.

Proof. The functors s_* commute with homotopy colimits [Spi08, Corollary 4.6]. Therefore, we can just invert h_1 in the description of $E_1(\mathbf{ko})$ given in Proposition 4.1 (see also Figure 5). \square

Remark 4.8. Table 5 gives an unexpected value for τ^2 . Recall that τ^2 is indecomposable in $E_1(\mathbf{ko})$, so there is no inconsistency. The unexpected value arises from Equation (1.1).

4.2. The Adams operation ψ^3 in effective spectral sequences. Our goal in this section is to study ψ^3 as a map of effective spectral sequences. This will allow us to compute the E_1 -page of the effective spectral sequence for L .

Lemma 4.9. *The map $E_\infty(\mathbf{ko}) \rightarrow E_\infty(\mathbf{ko})$ induced by ψ^3 on effective E_∞ -pages takes the values shown in Table 6.*

Proof. Corollary 2.4(2) gives the values of ψ^3 on ρ , h_1 , and τh_1 .

The value of ψ^3 on τ^4 is determined immediately by comparison along Betti realization to the classical value $\psi^3(1) = 1$. The computation is greatly simplified by ignoring terms in higher effective filtration. Similarly, the value of ψ^3 on $2\tau^2$ is determined by the classical value $\psi^3(2) = 2$.

The remaining values in Table 6 are also determined by comparison along Betti realization to the classical values $\psi^3(2v_1^2) = 9 \cdot 2v_1^2$ and $\psi^3(v_1^4) = 81v_1^4$. \square

Lemma 4.10. *The map $E_1(\mathbf{ko}) \rightarrow E_1(\mathbf{ko})$ induced by ψ^3 on effective E_1 -pages takes the values shown in Table 5.*

Proof. The values of ψ^3 on $E_1(\mathbf{ko})$ are compatible with the values of ψ^3 on $E_\infty(\mathbf{ko})$, as shown in Table 6. This immediately yields the value of ψ^3 on ρ , h_1 , and τh_1 .

The value of $\psi^3((\tau^2)^2)$ must be $(\tau^2)^2$ by compatibility with the value of $\psi^3(\tau^4)$ in $E_\infty(\mathbf{ko})$. Then the relation $\psi^3((\tau^2)^2) = (\psi^3(\tau^2))^2$ implies that $\psi^3(\tau^2) = \tau^2$.

Similarly, the value of $\psi^3((v_1^2)^2)$ must be $81(v_1^2)^2$ by compatibility with the value of $\psi^3(v_1^4)$ in $E_\infty(\mathbf{ko})$. Then the relation $\psi^3((v_1^2)^2) = (\psi^3(v_1^2))^2$ implies that $\psi^3(v_1^2) = 9v_1^2$. \square

Remark 4.11. Since ψ^3 is a ring homomorphism, all values of ψ^3 on $E_1(\mathbf{ko})$ are readily determined by the values on multiplicative generators given in Table 5. In particular, for all $k \geq 0$,

$$\psi^3(v_1^{2k}) = 9^k v_1^{2k}.$$

Remark 4.12. Table 5 implies that $\psi^3(v_1^4) = 81v_1^4$. The careful reader will notice that this expression appears to be simpler than the analogous formula in [BH20, Theorem 3.1(2)]. The difference is explained by the fact that we are working only up to higher filtration. In particular, our formulas do not reflect the difference between 2 and h. This also means that our formulas are less precise, but that has no consequence for our computational results.

5. THE EFFECTIVE SPECTRAL SEQUENCE FOR L

5.1. The effective E_1 -page of L . In this section we compute the E_1 -page of the effective spectral sequence for L .

The fiber sequence $L \rightarrow \mathbf{ko} \xrightarrow{\psi^3-1} \mathbf{ko}$ induces a fiber sequence

$$s_*L \rightarrow s_*\mathbf{ko} \xrightarrow{\psi^3-1} s_*\mathbf{ko}$$

on slices. Upon taking homotopy groups, we obtain a long exact sequence

$$\cdots \rightarrow E_1(L) \rightarrow E_1(\mathbf{ko}) \xrightarrow{\psi^3-1} E_1(\mathbf{ko}) \rightarrow \cdots.$$

Table 5 (see also Lemma 4.10) gives us complete computational knowledge of the map $E_1(\mathbf{ko}) \rightarrow E_1(\mathbf{ko})$. This allows us to compute $E_1(L)$.

Proposition 5.1. *The chart in Figure 10 depicts the effective E_1 -page of L .*

Proof. The long exact sequence

$$\cdots \rightarrow E_1(L) \rightarrow E_1(\mathbf{ko}) \xrightarrow{\psi^3-1} E_1(\mathbf{ko}) \rightarrow \cdots$$

induces a short exact sequence

$$0 \rightarrow \Sigma^{-1}C \rightarrow E_1(L) \rightarrow K \rightarrow 0,$$

where C and K are the cokernel and kernel of $E_1(\mathbf{ko}) \xrightarrow{\psi^3-1} E_1(\mathbf{ko})$. The cokernel and kernel can be computed directly from the information given in Lemma 4.10. See also Remark 4.11.

The kernel consists of all elements in $E_1(\mathbf{ko})$ with the exception of the integer multiples of $\tau^{2j} \cdot v_1^{2k}$ for $j \geq 0$ and $k > 0$.

The cokernel C is nearly the same as $E_1(\mathbf{ko})$ itself. We must impose the relations $(3^{2k} - 1)v_1^{2k} = 0$ for all $k > 0$. Lemma 3.8 says that $3^{2k} - 1$ equals $2^{v(2k)+2} \cdot u$, where u is an odd number, i.e., a unit in our 2-adic context. Therefore, the relation $(3^{2k} - 1)v_1^{2k} = 0$ is equivalent to the relation $2^{v(2k)+2}v_1^{2k} = 0$. \square

Table 8 lists some elements of the effective E_1 -page of L . In fact, by inspection these elements are multiplicative generators for $E_1(L)$.

We use the same notation for elements of $E_1(L)$ and their images in $E_1(\mathbf{ko})$. On the other hand, we define the element ιx of $E_1(L)$ to be the image of x under the

map $\iota : \Sigma^{-1}E_1(\text{ko}) \rightarrow E_1(L)$. For example, the element 1 of $E_1(\text{ko})$ maps to ι in $E_1(L)$.

Table 8: Multiplicative generators for $E_1(L)$: $k \geq 0$

coweight	(s, f, w)	generator	image in $E_1(L[\eta^{-1}])$
2	$(0, 0, -2)$	τ^2	$\tau^2 + \rho^2 \cdot v_1^2$
$2k + 1$	$(4k + 1, 1, 2k)$	$\tau h_1 v_1^{2k}$	$\tau(v_1^2)^k$
$2k$	$(4k - 1, 1, 2k - 1)$	ρv_1^{2k}	$\rho(v_1^2)^k$
$2k$	$(4k + 1, 1, 2k + 1)$	$h_1 v_1^{2k}$	$(v_1^2)^k$
$2k - 1$	$(4k - 1, 1, 2k)$	ιv_1^{2k}	$\iota(v_1^2)^k$

5.2. The effective spectral sequence for $L[\eta^{-1}]$. In Section 5.1, we determined the effective E_1 -page of L . The next steps in the analysis of the effective spectral sequence for L are to determine the multiplicative structure of $E_1(L)$ (see Section 5.3) and to determine the effective differentials (see Sections 5.4 and 5.5).

Before doing so, we collect some information on the η -periodicization $L[\eta^{-1}]$. We will study $L[\eta^{-1}]$ by comparing to the more easily understood $\text{ko}[\eta^{-1}]$.

As in Sections 3.3 and 4.1, powers of h_1 are inconsequential for computational purposes in the η -periodic context. Consequently, we have removed these powers from all η -periodic formulas.

Proposition 5.2. *The effective E_1 -page for $L[\eta^{-1}]$ is given by*

$$E_1(L[\eta^{-1}]) = \mathbb{F}_2[\tau, \rho, v_1^2, \iota]/\iota^2.$$

Moreover, the periodicization map $L \rightarrow L[\eta^{-1}]$ induces the map $E_1(L) \rightarrow E_1(L[\eta^{-1}])$ whose values are given in Table 8.

Proof. As in Proposition 4.7, we can just invert h_1 in the additive description of $E_1(L)$ given in Proposition 5.1.

The map $E_1(\text{ko}[\eta^{-1}]) \xrightarrow{\psi^3-1} E_1(\text{ko}[\eta^{-1}])$ is trivial because $(\psi^3 - 1)(h_1) = 0$, as shown in Table 5 (see also Lemma 4.10). Therefore, the long exact sequence

$$\cdots \longrightarrow E_1(L[\eta^{-1}]) \longrightarrow E_1(\text{ko}[\eta^{-1}]) \xrightarrow{\psi^3-1} E_1(\text{ko}[\eta^{-1}]) \longrightarrow \cdots$$

splits as

$$E_1(L[\eta^{-1}]) \cong E_1(\text{ko}[\eta^{-1}]) \oplus \Sigma^{-1}E_1(\text{ko}[\eta^{-1}]).$$

With Proposition 4.7, this establishes the additive structure of $E_1(L[\eta^{-1}])$, as well as most of the multiplicative structure.

The relation $\iota^2 = 0$ is immediate because there are no possible non-zero values for ι^2 . \square

Remark 5.3. As in Remark 4.8, Table 8 gives an unexpected value for τ^2 , which arises from Equation (1.1). Also, the last column of Table 8 leaves out of h_1 for readability.

Remark 5.4. Note that $E_1(L[\eta^{-1}])$ is very close to the effective E_1 -page for the η -periodic sphere $S[\eta^{-1}]$ [RSØ19, Theorem 2.32] [OR20, Theorem 2.3]. The element ι is not present in $E_1(S[\eta^{-1}])$, but the elements ιv_1^{2k} are present.

Proposition 5.5. *Some values of the differentials in the effective spectral sequence of $L[\eta^{-1}]$ are:*

$$(1) d_1(v_1^2) = \tau.$$

$$(2) d_{n+1}(v_1^{2n}) = \rho^{n+1} \cdot \iota v_1^{2n} \text{ for } n \geq 2.$$

The effective differentials are zero on all other multiplicative generators on all pages.

Following our convention throughout this section, we have omitted the powers of h_1 from the formulas in Proposition 5.5.

Proof. The d_1 differential follows from [RSØ19, Lemma 4.2] or [OR20, Theorem 2.6].

To study the higher differentials, consider the map $S[\eta^{-1}] \rightarrow L[\eta^{-1}]$. This map induces an isomorphism on stable homotopy groups, except in coweight -1 . This follows from a minor adjustment to [BH20, Theorem 1.1]. The adjustment arises from the fact that our $L[\eta^{-1}]$ is the fiber of $\text{ko}[\eta^{-1}] \xrightarrow{\psi^3-1} \text{ko}[\eta^{-1}]$, while [BH20, Theorem 1.1] refers to the fiber of $\text{ko}[\eta^{-1}] \xrightarrow{\psi^3-1} \Sigma^{8,4}\text{ko}[\eta^{-1}]$.

The homotopy of $S[\eta^{-1}]$ is completely computed in [GI16], so the homotopy of $L[\eta^{-1}]$ is known (except in coweight -1). There is only one pattern of differentials that is compatible with the known values for $L[\eta^{-1}]$. \square

Remark 5.6. In the language of [OR20, Section 4], Proposition 5.5 establishes the profile of the η -periodic effective spectral sequence over \mathbb{R} .

5.3. Multiplicative relations for $E_1(L)$. In this section, we will completely describe the product structure on $E_1(L)$. We do not need all of this structure for our later computations, but we include it for completeness.

Proposition 5.7. *Table 9 lists some products in $E_1(L)$.*

Table 9: Products in $E_1(L)$: $j \geq 0$ and $k \geq 0$

	ρv_1^{2j}	$h_1 v_1^{2j}$	$\tau h_1 v_1^{2j}$	ιv_1^{2j}
ρv_1^{2k}	$\rho \cdot \rho v_1^{2j+2k}$			
$h_1 v_1^{2k}$	$\rho \cdot h_1 v_1^{2j+2k}$	$h_1 \cdot h_1 v_1^{2j+2k}$		
$\tau h_1 v_1^{2k}$	$\rho \cdot \tau h_1 v_1^{2j+2k}$	$h_1 \cdot \tau h_1 v_1^{2j+2k}$	$\tau^2 \cdot h_1 \cdot h_1 v_1^{2j+2k} +$	

Table 9: Products in $E_1(L)$: $j \geq 0$ and $k \geq 0$

	ρv_1^{2j}	$h_1 v_1^{2j}$	$\tau h_1 v_1^{2j}$	ιv_1^{2j}
			$+\rho \cdot \rho v_1^{2j+2k+2}$	
ιv_1^{2k}	$\rho \cdot \iota v_1^{2j+2k}$	$h_1 \cdot \iota v_1^{2j+2k}$	$\tau h_1 \cdot \iota v_1^{2j+2k}$	0

Proof. All of these products are detected by $E_1(L[\eta^{-1}])$, which is described in Proposition 5.2. We need the values of the periodicization map $E_1(L) \rightarrow E_1(L[\eta^{-1}])$ given in Table 8. \square

5.4. **The effective d_1 differential for L .** Our next task is to compute the differentials in the effective spectral sequence for L .

Proposition 5.8. *Table 10 gives the values of the effective d_1 differential on the multiplicative generators of $E_1(L)$.*

Table 10: Effective d_1 differentials for L : $k \geq 0$

coweight	(s, f, w)	x	$d_1(x)$
2	$(0, 0, -2)$	τ^2	$\rho^2 \cdot \tau h_1$
$4k$	$(8k - 1, 1, 4k - 1)$	ρv_1^{4k}	
$4k + 2$	$(8k + 3, 1, 4k + 1)$	ρv_1^{4k+2}	$\rho h_1^2 \cdot \tau h_1 v_1^{4k}$
$4k$	$(8k + 1, 1, 4k + 1)$	$h_1 v_1^{4k}$	
$4k + 2$	$(8k + 5, 1, 4k + 3)$	$h_1 v_1^{4k+2}$	$h_1^3 \cdot \tau h_1 v_1^{4k}$
$4k + 3$	$(8k + 5, 1, 4k + 2)$	$\tau h_1 v_1^{4k+2}$	$\tau^2 \cdot h_1^3 \cdot h_1 v_1^{4k} + \rho^2 h_1 \cdot h_1 v_1^{4k+2}$
$4k + 1$	$(8k + 1, 1, 4k)$	$\tau h_1 v_1^{4k}$	
$4k + 1$	$(8k + 3, 1, 4k + 2)$	ιv_1^{4k+2}	$\tau h_1 \cdot h_1^2 \cdot \iota v_1^{4k}$
$4k - 1$	$(8k - 1, 1, 4k)$	ιv_1^{4k}	

Proof. All of these differentials follow immediately from the effective d_1 differentials for $L[\eta^{-1}]$, which are all determined by Proposition 5.5(1). Beware that the exact values of the map $E_1(L) \rightarrow E_1(L[\eta^{-1}])$, as shown in Table 8, are important.

For example, consider the differential on the element $\tau h_1 v_1^{4k+2}$. It maps to $\tau(v_1^2)^{2k+1}$ in $E_1(L[\eta^{-1}])$ (up to h_1 multiples, which as usual we ignore in the η -periodic situation). The η -periodic differential on this latter element is $\tau^2(v_1^2)^{2k}$. Finally, we need to find an element of $E_1(L)$ in the correct degree whose η -periodicization is $\tau^2(v_1^2)^{2k}$. The only possibility is $\tau^2 \cdot h_1^3 \cdot h_1 v_1^{4k} + \rho^2 h_1 \cdot h_1 v_1^{4k+2}$. \square

Remark 5.9. All d_1 differentials in $E_1(L)$ can be deduced from the information in Table 10 and the Leibniz rule, but the computations can be complicated by the multiplicative relations of Table 9. For example,

$$d_1(\tau^2 \cdot \tau h_1 v_1^2) = \rho^2 \cdot \tau h_1 \cdot \tau h_1 v_1^2 + \tau^2(\tau^2 \cdot h_1^4 + \rho^2 h_1 \cdot h_1 v_1^2) = \tau^4 \cdot h_1^4 + \rho^4 \cdot v_1^4.$$

Having completely analyzed the slice d_1 differentials for $E_1(L)$, it is now possible to compute the E_2 -page of the slice spectral sequence for L .

Proposition 5.10. *The E_2 -page of the effective spectral sequence for L is depicted in Figures 11, 12, 14, and 15.*

For legibility, Figures 11, 12, 14, and 15 display $E_2(L)$ in four different charts separated by coweight modulo 4. Note that Figures 14 and 15 also serve as E_∞ -page charts in coweights 1 and 2 modulo 4 because there are no higher differentials that affect these coweights.

Proof. The Leibniz rule, together with the values in Table 10, completely determines the effective d_1 differential on $E_1(L)$. The E_2 -page can then be determined directly. However, as in the proof of Theorem 4.3, the computation is not entirely straightforward.

It turns out that the d_1 differential preserves the image of the map $\Sigma^{-1}E_1(\text{ko}) \rightarrow E_1(L)$. Moreover, it turns out that all d_1 differentials with values in the image of $\Sigma^{-1}E_1(\text{ko}) \rightarrow E_1(L)$ also have source in this image. (This is not for formal reasons; in fact, the higher effective differentials do not have this property.) Consequently, the determination of the E_2 -page splits into two separate computations: one for the image of $\Sigma^{-1}E_1(\text{ko}) \rightarrow E_1(L)$, and one for the cokernel of the same map.

In more concrete terms, we can determine $E_2(L)$ by first considering only elements of the form ιx , and then separately considering only elements that are not of this form.

The d_1 differential on the image of $\Sigma^{-1}E_1(\text{ko}) \rightarrow E_1(L)$ is identical to the d_1 differential for ko discussed in Section 4. The d_1 differential on the cokernel of $\Sigma^{-1}E_1(\text{ko}) \rightarrow E_1(L)$ is similar to the d_1 differential on $E_1(\text{ko})$, but slightly different. The difference is created by the absence of the elements v_1^{2k} in $E_1(L)$. \square

5.5. Higher differentials. We now consider the higher differentials in the effective spectral sequence for L .

By inspection of the charts for $E_2(L)$, the only possible higher differentials have source in coweight congruent to 0 modulo 4 and value in coweight congruent to 3 modulo 4. In other words, in coweights congruent to 1 and 2 modulo 4, we have that $E_2(L)$ equals $E_\infty(L)$.

It turns out that there are many higher differentials. In fact, nearly all of the elements in $E_2(L)$ in coweight congruent to 0 modulo 4 support differentials. While it is possible to write down explicit formulas for all of these differentials, the formulas would be cumbersome and not so helpful. Rather, we give a more qualitative description of the differentials because it is more useful for computation.

Proposition 5.11. *Consider the elements of $E_2(L)$ in coweights congruent to 0 modulo 4 that belong to the cokernel of the map $\Sigma^{-1}E_2(\text{ko}) \rightarrow E_2(L)$.*

- (1) The only permanent cycles are the multiples of 1, the multiples of $2\tau^{4k}$ for $k \geq 0$, and $\rho^a h_1^b$ for all $a \geq 0$ and $b \geq 0$.
- (2) Excluding the elements listed in (1), if an element has coweight congruent to 2^{r-1} modulo 2^r , then it supports a d_r differential.

Proposition 5.11 may seem imprecise because it does not give the values of the differentials. However, there is only one non-zero possible value in every case, so there is no ambiguity.

Proof. These differentials follow immediately from the η -periodic differentials of Proposition 5.5, together with multiplicative relations in $E_2(L)$.

For example, consider the element $\tau^8 \cdot \rho v_1^{12}$ in coweight 20, which is congruent to 2^2 modulo 2^3 . Using Table 8, we find that this element maps to $\rho^9 (v_1^2)^{10}$ in $E_2(L[\eta^{-1}])$. Here we are using that τ^2 is zero in $E_2(L[\eta^{-1}])$ since it is hit by an η -periodic d_1 differential. Proposition 5.5 says that this element supports an η -periodic d_3 differential. It follows that $\tau^8 \cdot \rho v_1^{12}$ also supports a d_3 differential. \square

Theorem 5.12. *The E_∞ -page of the effective spectral sequence for L is depicted in Figures 13, 14, 15, 16, 17, 18, and 19.*

Proof. The E_∞ -page can be deduced directly from the higher differentials described in Proposition 5.11. \square

The E_∞ -page in coweights congruent to 3 modulo 4 is by far the most complicated case. Figures 17, 18, and 19 display $E_\infty(L)$ in coweights congruent to 3 modulo 8, 7 modulo 16, and 15 modulo 32 respectively.

In each case (and more generally in coweights congruent to $2^{n-1} - 1$ modulo 2^n), we see similar patterns with minor variations. The lower boundary of each chart takes the same shape. The upper boundary of the τ -periodic portion of each chart also takes the same shape. However, the filtration jump between the lower and upper boundaries increases linearly with n .

In addition to the τ -periodic portion of each chart, there are also τ -torsion, η -periodic regions. These consist of bands of infinite h_1 -towers of width n that repeat every 2^{n+1} stems. The first such band starts at $\nu v_1^{2^{n-1}}$.

5.6. Hidden extensions. Our last goal is to compute hidden extensions by ρ , h , and η . See [Isa19, Section 4.1] for a precise definition of a hidden extension. Fortunately, none of the complications associated with crossing extensions occur in this manuscript.

Proposition 5.13. *Table 11 lists some hidden extensions by ρ , h , and η in the effective spectral sequence for L .*

Proof. The last column of Table 11 indicates the reason for each hidden extension. Some of the hidden extensions follow from the analogous extensions for ko given in Table 7, using the maps $\Sigma^{-1}ko \rightarrow L$ and $L \rightarrow ko$.

Other extensions follow from the long exact sequence associated to the cofiber sequence

$$\Sigma^{-1,-1}L \xrightarrow{\rho} L \longrightarrow L/\rho.$$

Here we need that the homotopy of L/ρ is isomorphic to the homotopy of $L^{\mathbb{C}}$, as shown in Proposition 2.9. For example, the hidden h extensions of Proposition 3.16 give hidden h extensions in L/ρ , which then imply the hidden extension from $\iota 4v_1^2$ to $h_1^2 \cdot \tau h_1$. □

Table 11: Hidden extensions in $E_{\infty}(L)$

coweight	source	type	target	(s, f, w)	proof
0	$\iota \cdot \tau h_1$	h	$\iota \cdot \rho h_1 \cdot \tau h_1$	$(0, 2, 0)$	$\Sigma^{-1}\text{ko} \rightarrow L$
1	τh_1	h	$\rho h_1 \cdot \tau h_1$	$(1, 1, 0)$	$L \rightarrow \text{ko}$
1	$\iota(\tau h_1)^2$	h	$\iota \cdot \rho h_1(\tau h_1)^2$	$(1, 3, 0)$	$\Sigma^{-1}\text{ko} \rightarrow L$
1	$\iota \cdot 2\tau^2$	η	$\iota \cdot \rho(\tau h_1)^2$	$(-1, 1, -2)$	$\Sigma^{-1}\text{ko} \rightarrow L$
1	$\iota 2v_1^2$	ρ	$\iota \cdot h_1(\tau h_1)^2$	$(3, 1, 2)$	$\Sigma^{-1}\text{ko} \rightarrow L$
1	$\iota 4v_1^2$	h	$h_1^2 \cdot \tau h_1$	$(3, 1, 2)$	L/ρ
2	$(\tau h_1)^2$	h	$\rho h_1(\tau h_1)^2$	$(2, 2, 0)$	$L \rightarrow \text{ko}$
3	$\iota 4\tau^2 v_1^2$	h	$(\tau h_1)^3$	$(3, 1, 0)$	L/ρ
3	$\iota 2\tau^2 v_1^2$	ρ	$\iota \tau^4 \cdot h_1^3$	$(3, 1, 0)$	$\Sigma^{-1}\text{ko} \rightarrow L$
3	$\iota 2\tau^2 v_1^2$	η	$\rho^3 \cdot \iota v_1^4$	$(3, 1, 0)$	$\Sigma^{-1}\text{ko} \rightarrow L$
2	$2\tau^2$	η	$\rho(\tau h_1)^2$	$(0, 0, -2)$	$L \rightarrow \text{ko}$
3	$(\tau h_1)^3$	h	$\iota \tau^4 \cdot \rho^2 h_1^6$	$(3, 3, 0)$	L/ρ
5	$\iota v_1^4 \cdot 8\tau^2$	h	$\rho^2 \cdot \tau h_1 v_1^4$	$(7, 1, 2)$	L/ρ

Remark 5.14. The hidden extensions in Table 11 are τ^4 -periodic in the following sense. If we take the source and target of each extension in $E_1(L)$ and multiply by τ^4 , then we obtain permanent cycles that are related by a hidden extension. For example, the hidden h extension from τh_1 to $\rho h_1 \cdot \tau h_1$ generalizes to a family of hidden extensions from $\tau^{4k+1}h_1$ to $\rho h_1 \cdot \tau^{4k+1}h_1$ for all $k \geq 0$.

Remark 5.15. Similarly to the τ^4 -periodicity discussed in Remark 5.14, most of the hidden extensions in Table 11 are v_1^4 -periodic as well. For example, the hidden h extension from τh_1 to $\rho h_1 \cdot \tau h_1$ generalizes to a family of hidden extensions from $\tau h_1 v_1^{4k}$ to $\rho h_1 \cdot \tau h_1 v_1^{4k}$ for all $k \geq 0$. There are three exceptions, which appear below

the horizontal divider at the bottom of the table. These exceptions are discussed in more detail in Remarks 5.16, 5.17, and 5.18.

Remark 5.16. The hidden η extension from $2\tau^2$ to $\rho(\tau h_1)^2$ is τ^4 -periodic as in Remark 5.14, but it is not v_1^4 -periodic. The elements $2\tau^2 v_1^{4k}$ are not permanent cycles for $k \geq 1$.

Remark 5.17. The hidden h extension from $\iota v_1^4 \cdot 8\tau^2$ to $\rho^2 \cdot \tau h_1 v_1^4$ is v_1^4 -periodic, but the situation is slightly more complicated than in Remark 5.15. For all k , $\rho^2 \cdot \tau h_1 v_1^{4k}$ receives a hidden h extension from an appropriate multiple of $\iota v_1^{4k} \cdot 2\tau^2$. For example, as shown in Figure 14, there is a hidden h extension from $\iota v_1^{4k} \cdot 16\tau^2$ to $\rho^2 \cdot \tau h_1 v_1^8$.

Remark 5.18. The hidden h extension from $(\tau h_1)^3$ to $\iota \tau^4 \cdot \rho^2 h_1^6$ is v_1^4 -periodic, but the situation is more complicated than in Remarks 5.15 and 5.17. For all $k \geq 0$, the element $(\tau h_1)^2 \tau h_1 v_1^{4k}$ supports a hidden h extension to the element of $E_\infty(L)$ of highest filtration in the appropriate degree. For example, as shown in Figure 18, there is a hidden h extension from $(\tau h_1)^2 \cdot \tau^5 h_1$ to $\iota \tau^8 \cdot \rho^3 h_1^7$. Figures 17, 18, and 19 show several extensions of this type.

6. CHARTS

We explain the notation used in the charts.

- The horizontal coordinate is the stem s . The vertical coordinate is the Adams-Novikov filtration f (see Section 1.7 for further discussion).
- Black or green circles represent copies of \mathbb{F}_2 , periodicized by some power of τ . The relevant power of τ varies from chart to chart.
- Black or green unfilled boxes represent copies of \mathbb{Z} (the 2-adic integers), periodicized by some power of τ . The relevant power of τ varies from chart to chart.
- Black or green boxes containing a number n represent copies of $\mathbb{Z}/2^n$, periodicized by some power of τ . The relevant power of τ varies from chart to chart.
- Red unfilled boxes represent copies of \mathbb{Z} (the 2-adic integers) that are not τ^k -periodic for any k .
- Green objects represent elements in the image of the map $\Sigma^{-1}\mathrm{ko} \rightarrow L$ (or $\Sigma^{-1}\mathrm{ko}^{\mathbb{C}} \rightarrow L^{\mathbb{C}}$).
- Black objects represent elements in the cokernel of the map $\Sigma^{-1}\mathrm{ko} \rightarrow L$ (or $\Sigma^{-1}\mathrm{ko}^{\mathbb{C}} \rightarrow L^{\mathbb{C}}$). In other words, they are detected by the map $L \rightarrow \mathrm{ko}$ (or $L^{\mathbb{C}} \rightarrow \mathrm{ko}^{\mathbb{C}}$).
- Lines of slope 1 represent h_1 -multiplications.
- Black or green arrows of slope 1 represent infinite sequences of elements that are τ^k -periodic for some $k > 0$ and are connected by h_1 -multiplications.

- Red arrows of slope 1 represent infinite sequences of elements that are connected by h_1 -multiplications and are not τ^k -periodic for any k .
- Lines of slope -1 represent ρ -multiplications.
- Dashed lines of slope -1 represent ρ -multiplications whose values are multiples of τ^k for some $k > 0$. For example, in Figure 6, we have $\rho \cdot \rho^3 v_1^4$ equals $\tau^4 \cdot h_1^4$.
- Black or green arrows of slope -1 represent infinite sequences of elements that are τ^k -periodic for some $k > 0$ and are connected by ρ -multiplications.
- Light blue lines of slope -3 represent effective d_1 differentials.
- Dashed light blue lines of slope -3 represent effective d_1 differentials that hit multiples of τ^k , for some $k > 0$. For example, the dashed line in Figure 1 indicates that $d_1(v_1^2)$ equals τh_1^3 .
- Dark blue lines indicate hidden extensions by h , ρ , or h_1 .
- Dashed dark blue lines indicate hidden extensions whose value is a multiple of τ^k for some $k > 0$. For example, in Figure 4, there is a hidden h extension from $\iota A v_1^2$ to τh_1^3 .

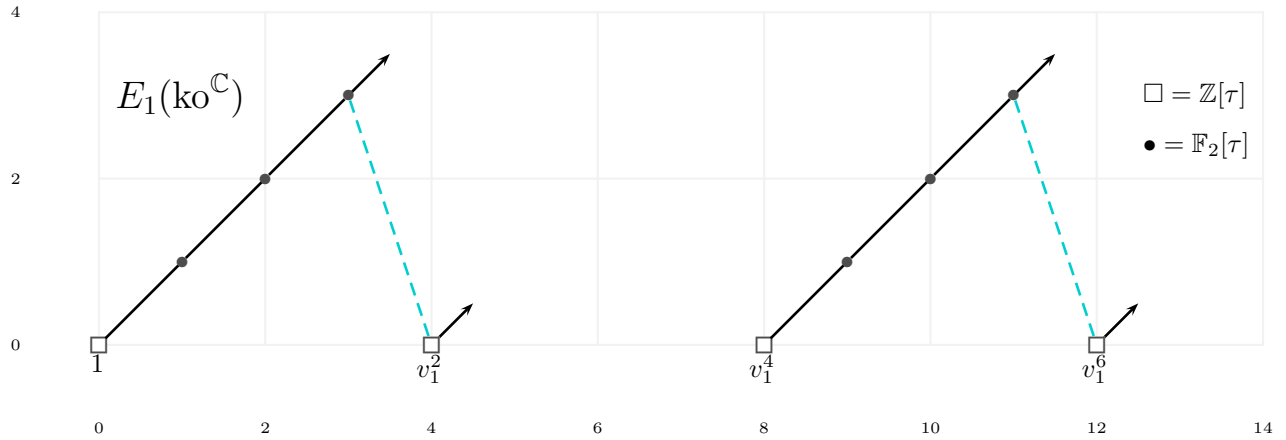


FIGURE 1. The E_1 -page of the effective spectral sequence for $\text{ko}^{\mathbb{C}}$

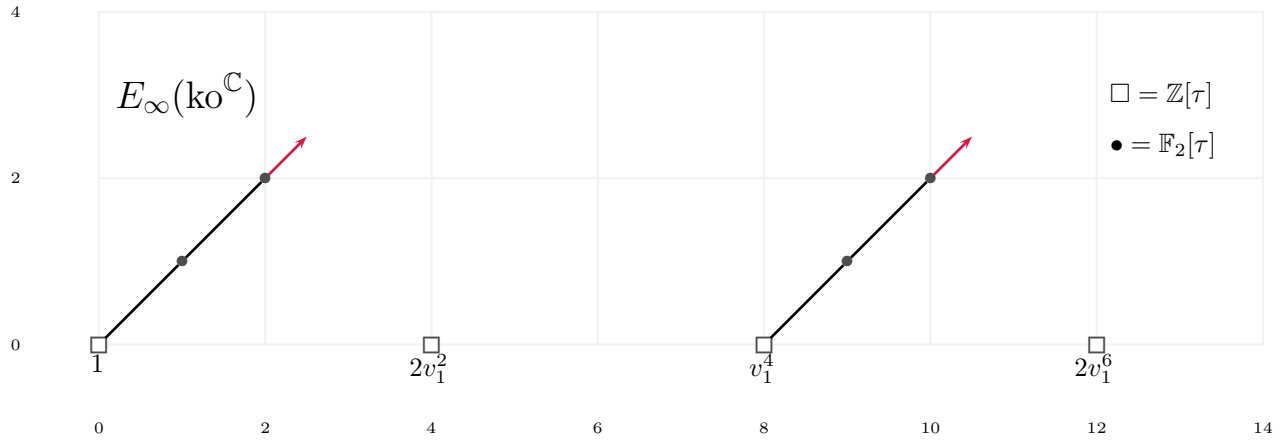


FIGURE 2. The E_∞ -page of the effective spectral sequence for $ko^{\mathbb{C}}$

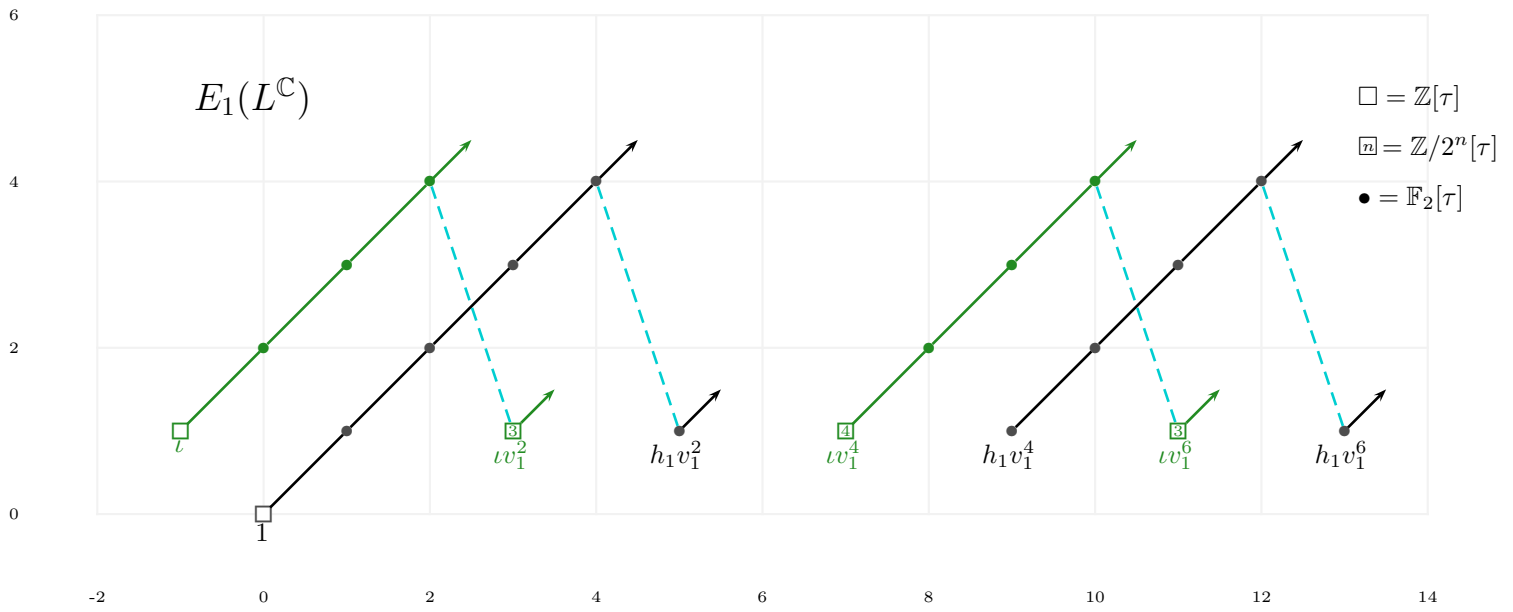


FIGURE 3. The E_1 -page of the effective spectral sequence for $L^{\mathbb{C}}$

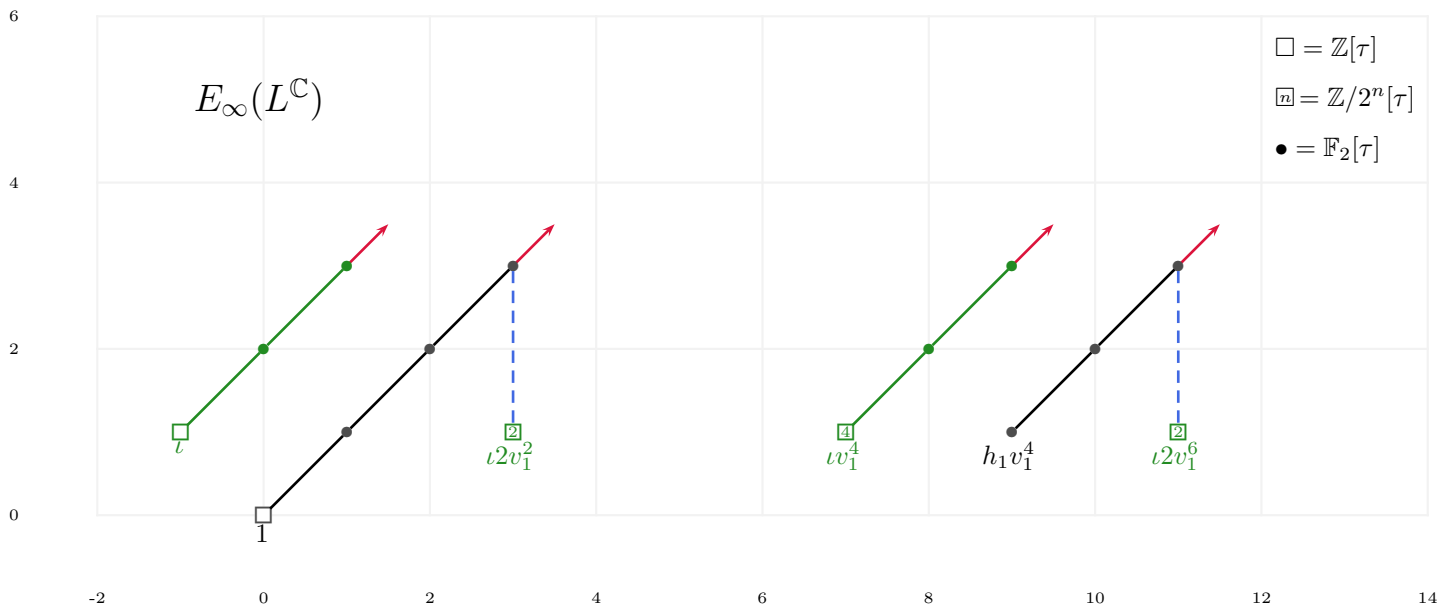


FIGURE 4. The E_∞ -page of the effective spectral sequence for L^C

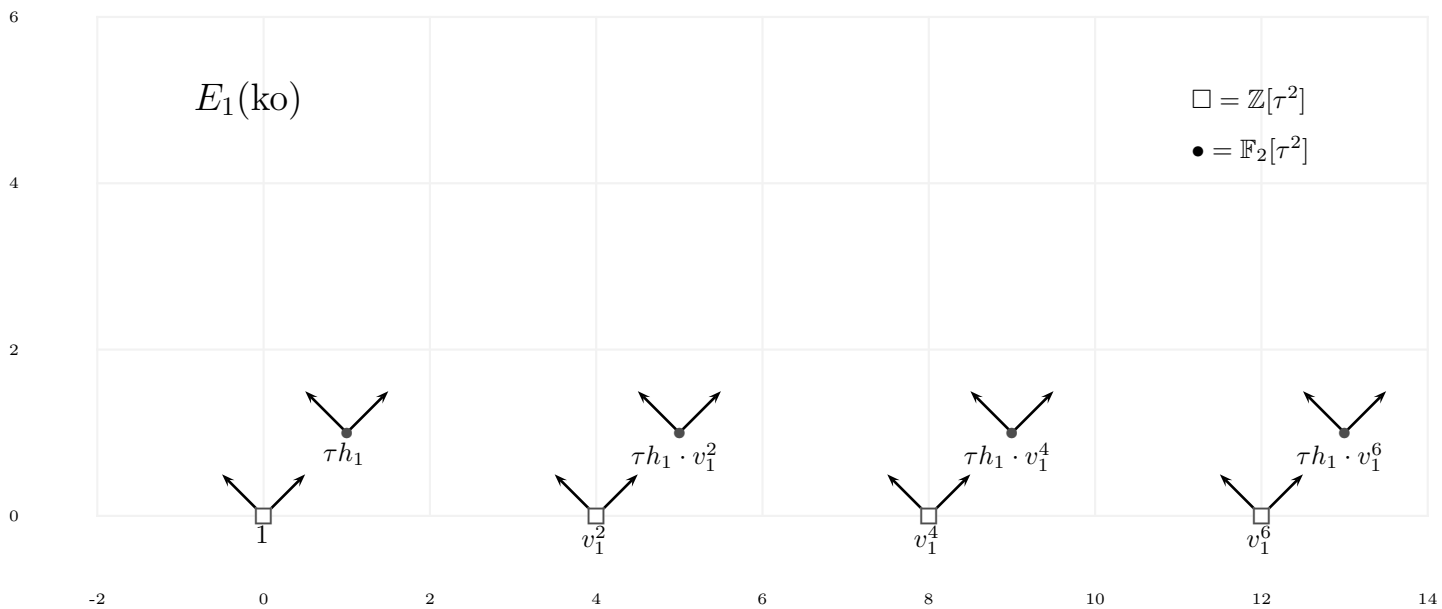


FIGURE 5. The E_1 -page of the effective spectral sequence for ko

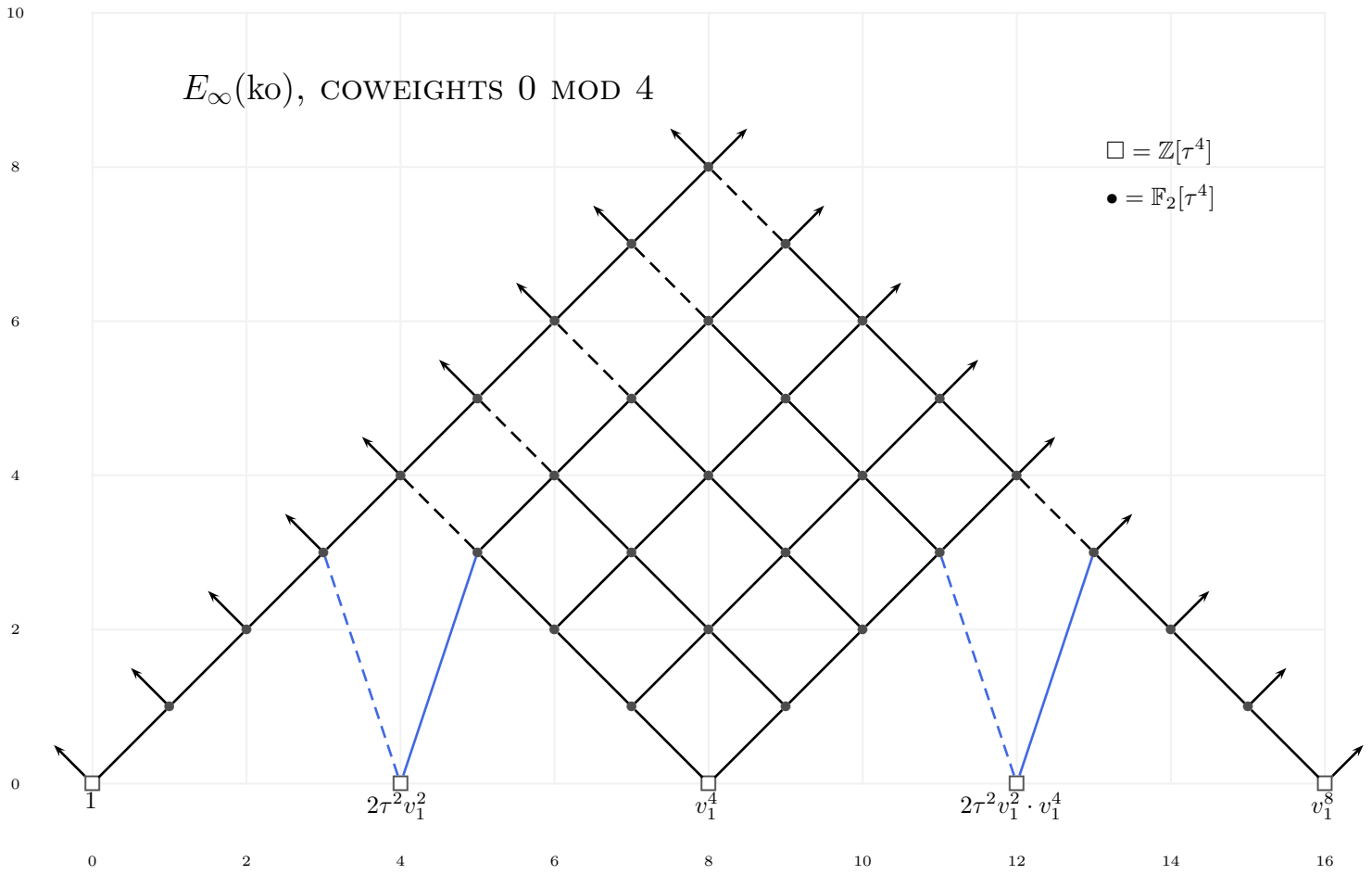


FIGURE 6. The E_∞ -page of the effective spectral sequence for ko in coweights $0 \pmod 4$

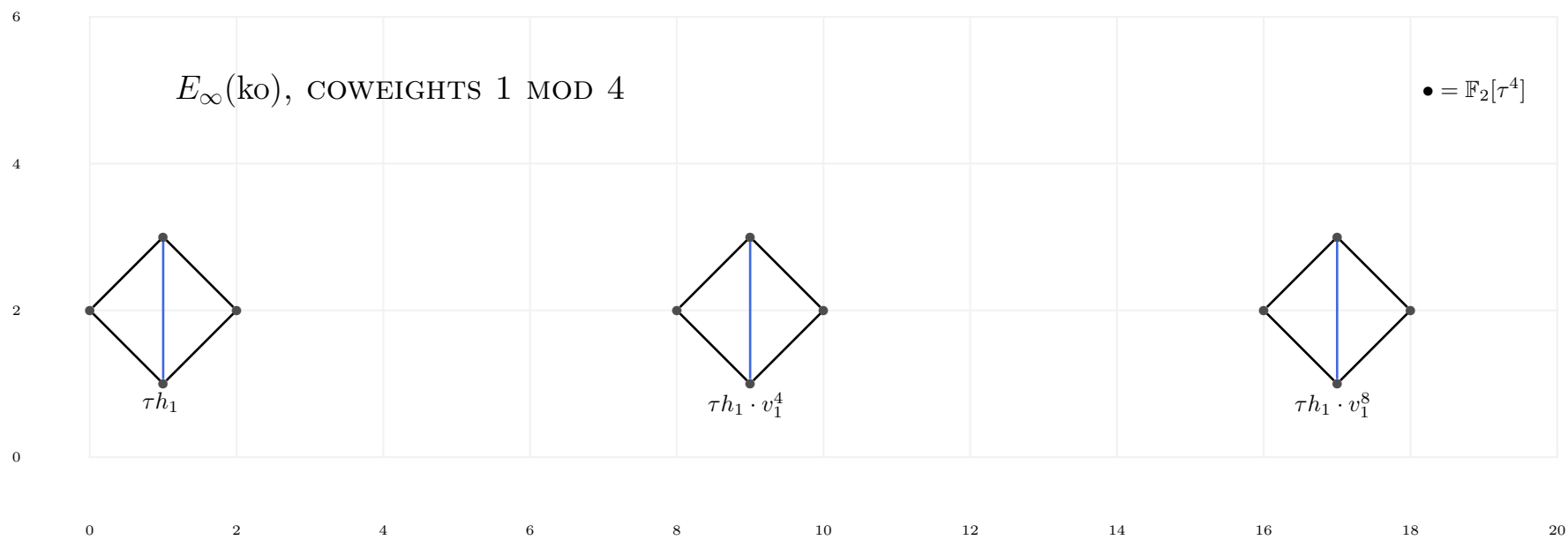


FIGURE 7. The E_∞ -page of the effective spectral sequence for ko in coweights 1 mod 4

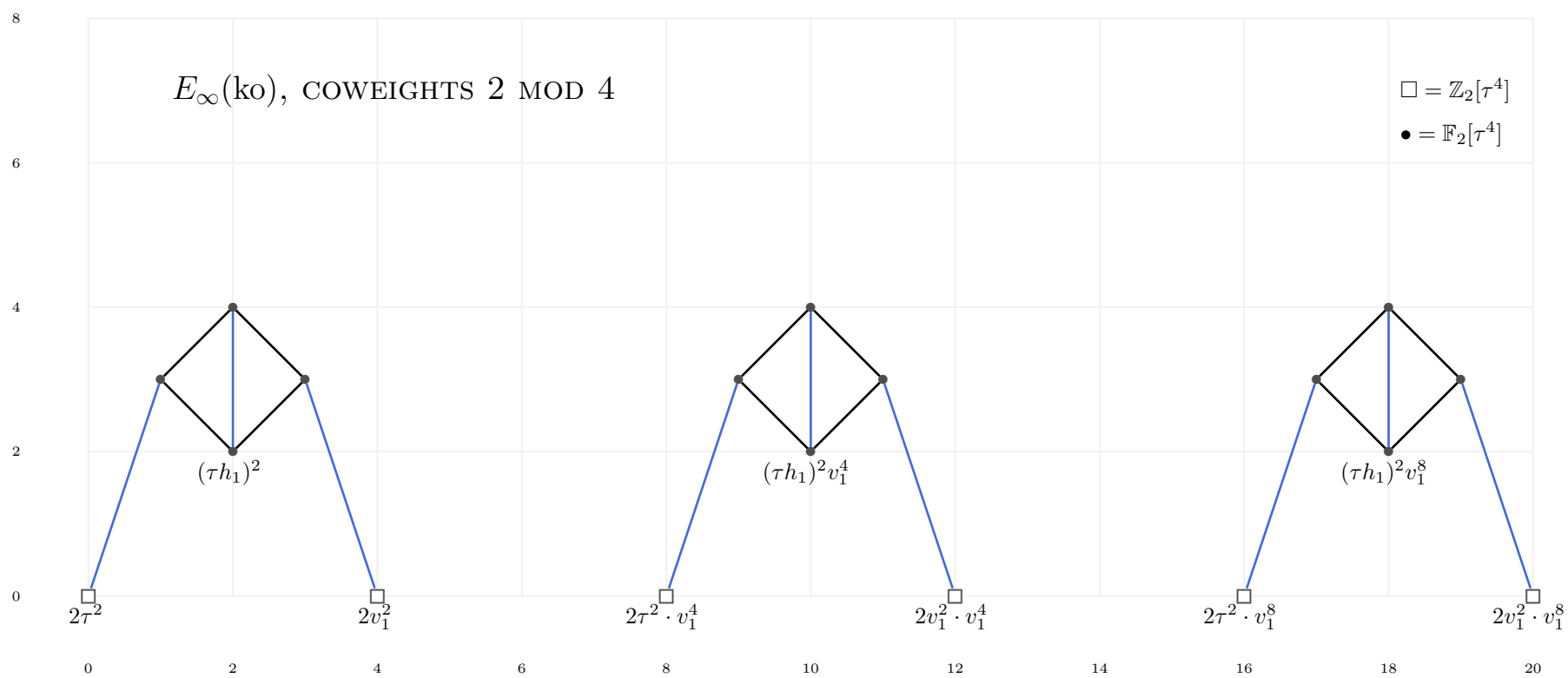


FIGURE 8. The E_∞ -page of the effective spectral sequence for ko in coweights 2 mod 4

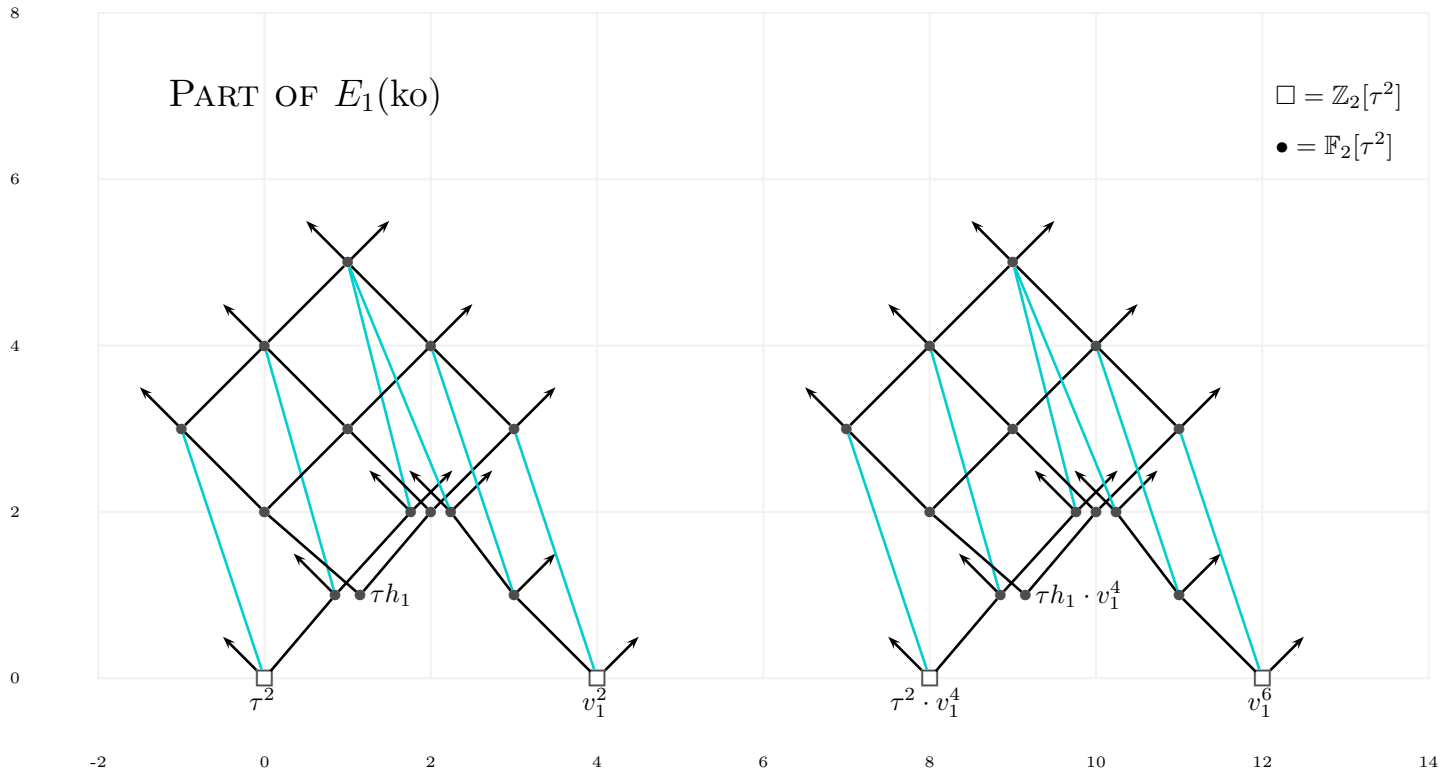


FIGURE 9. Some differentials in the effective spectral sequence for k_0

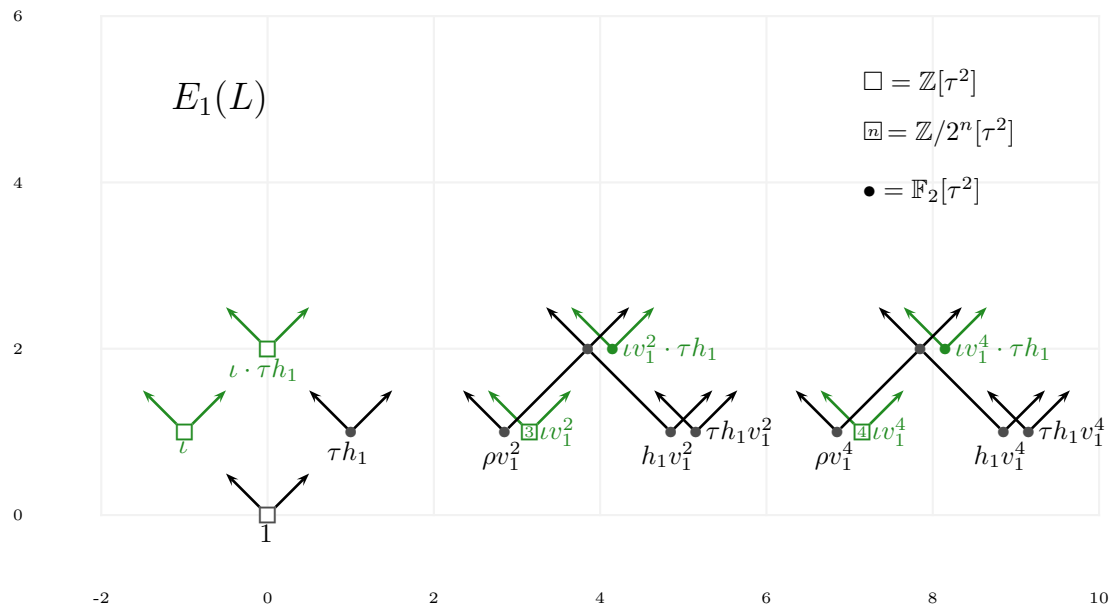


FIGURE 10. The E_1 -page of the effective spectral sequence for L

$E_2(L)$ IN COWEIGHTS 0 MOD 4

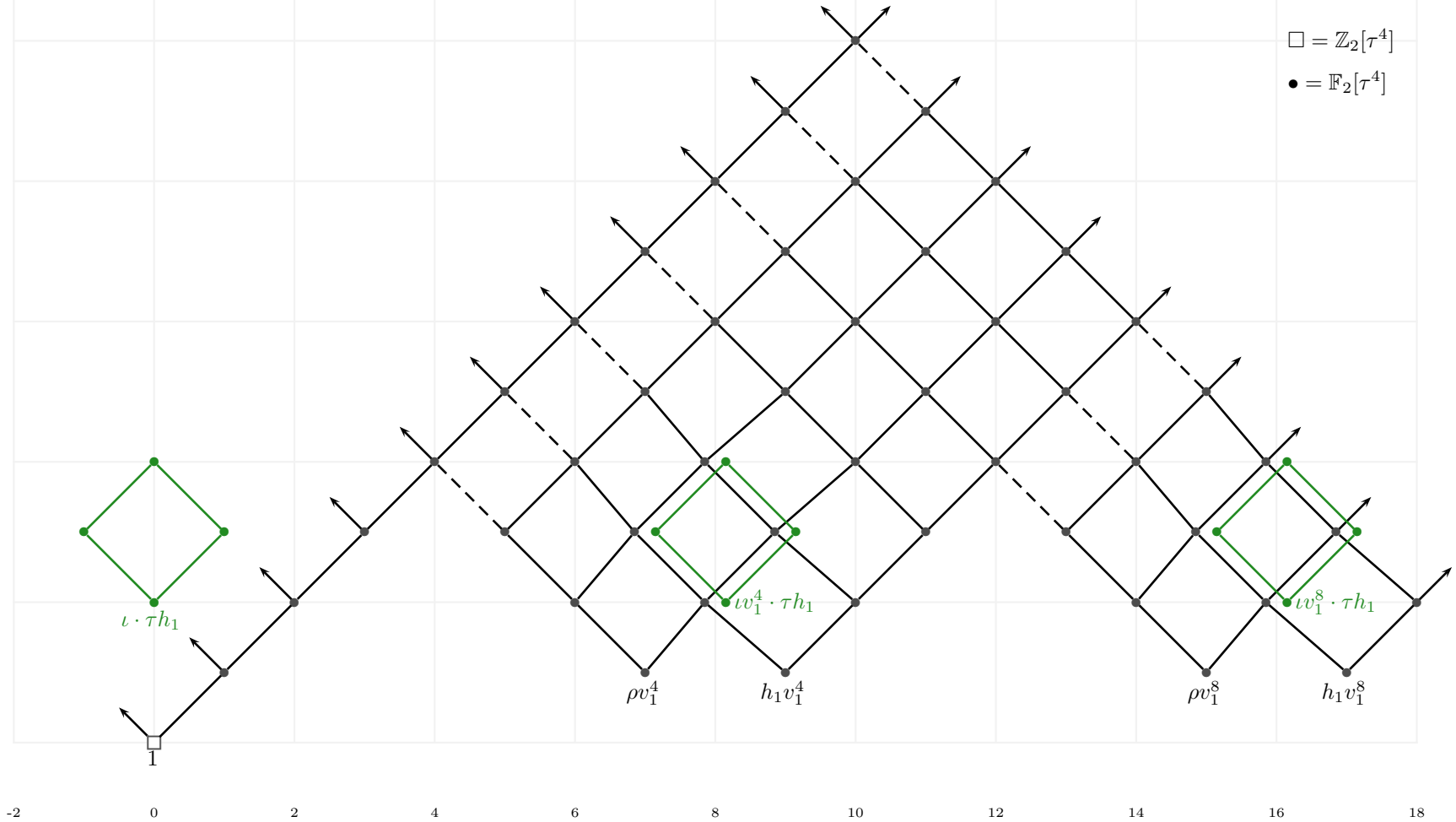


FIGURE 11. The E_2 -page of the effective spectral sequence for L in coweights 0 mod 4

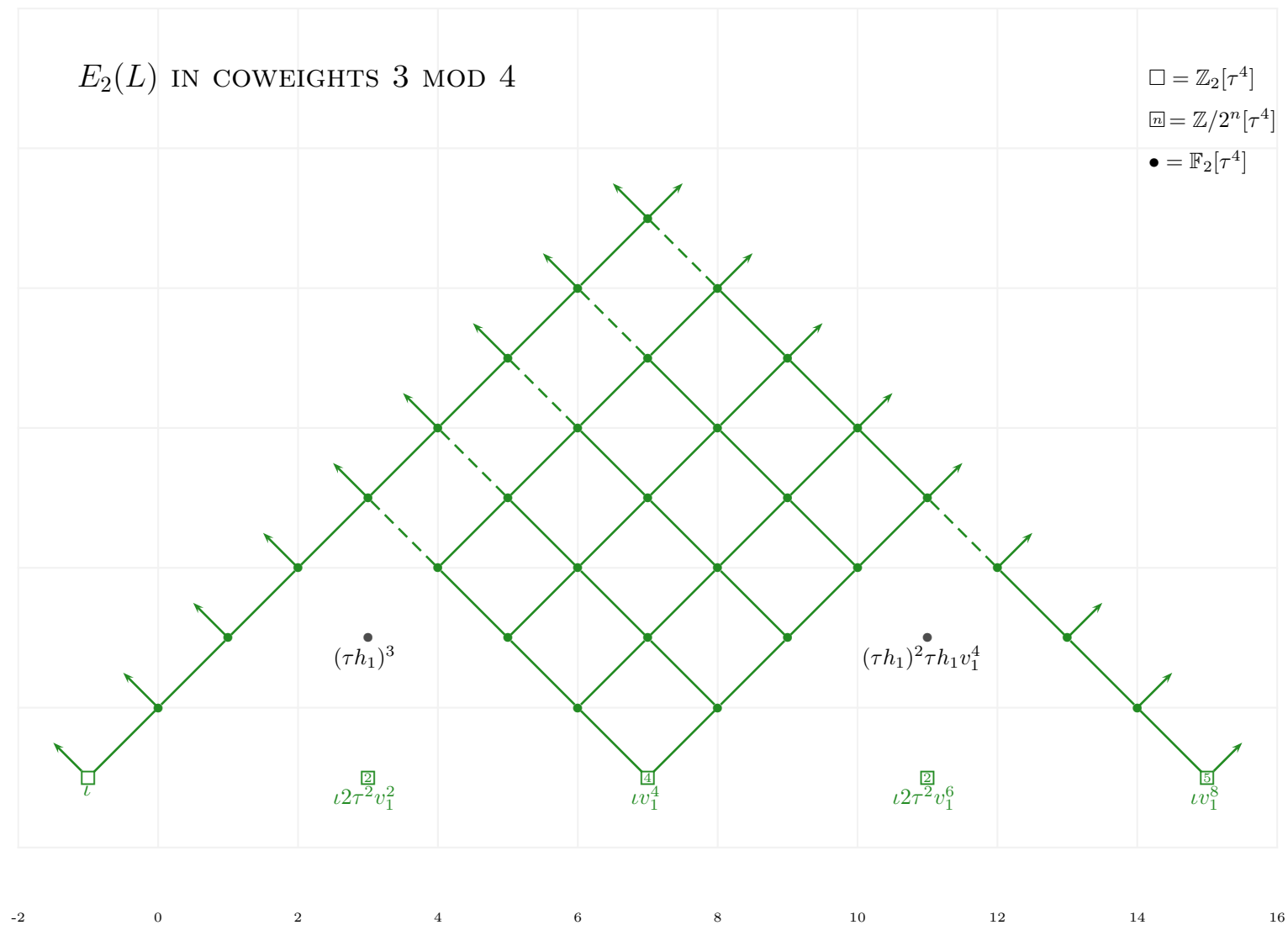


FIGURE 12. The E_2 -page of the effective spectral sequence for L in coweights 3 mod 4

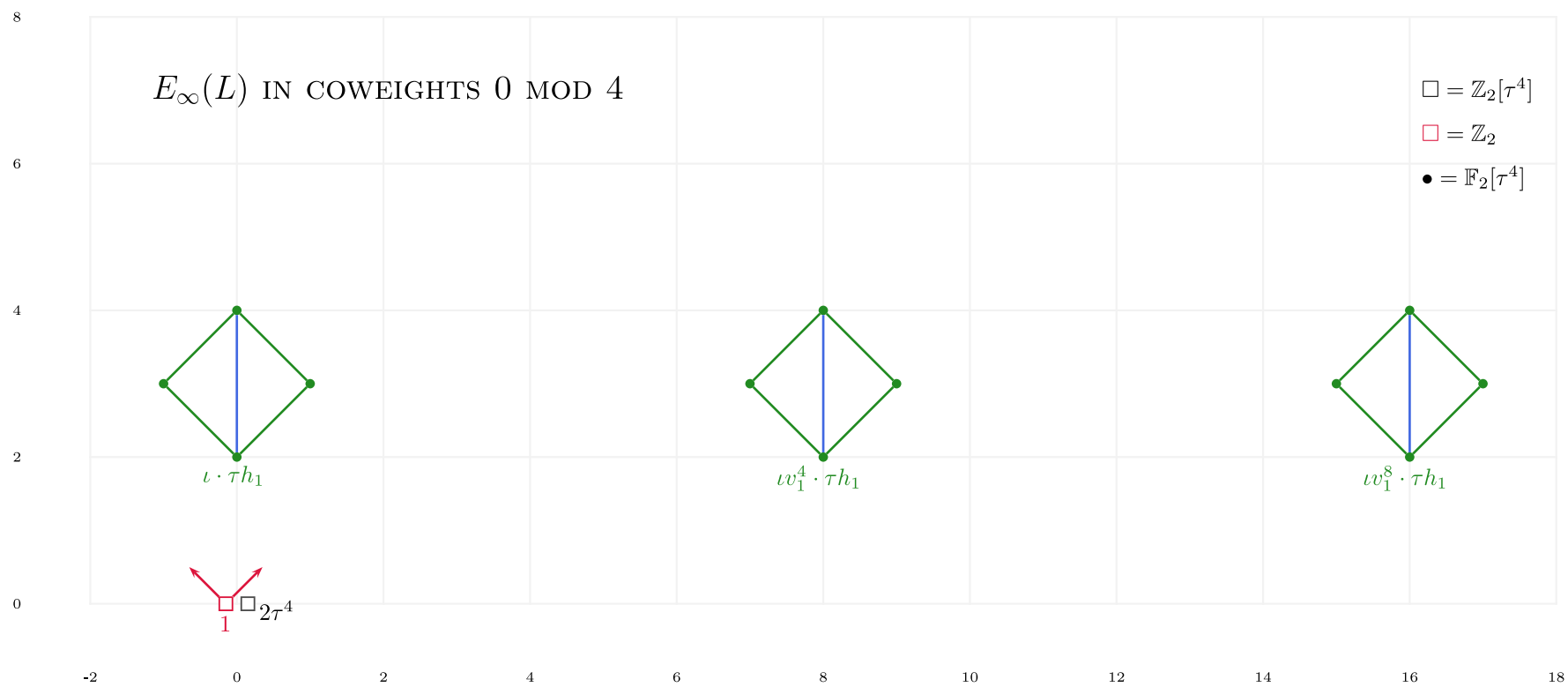


FIGURE 13. The E_∞ -page of the effective spectral sequence for L in coweights 0 mod 4

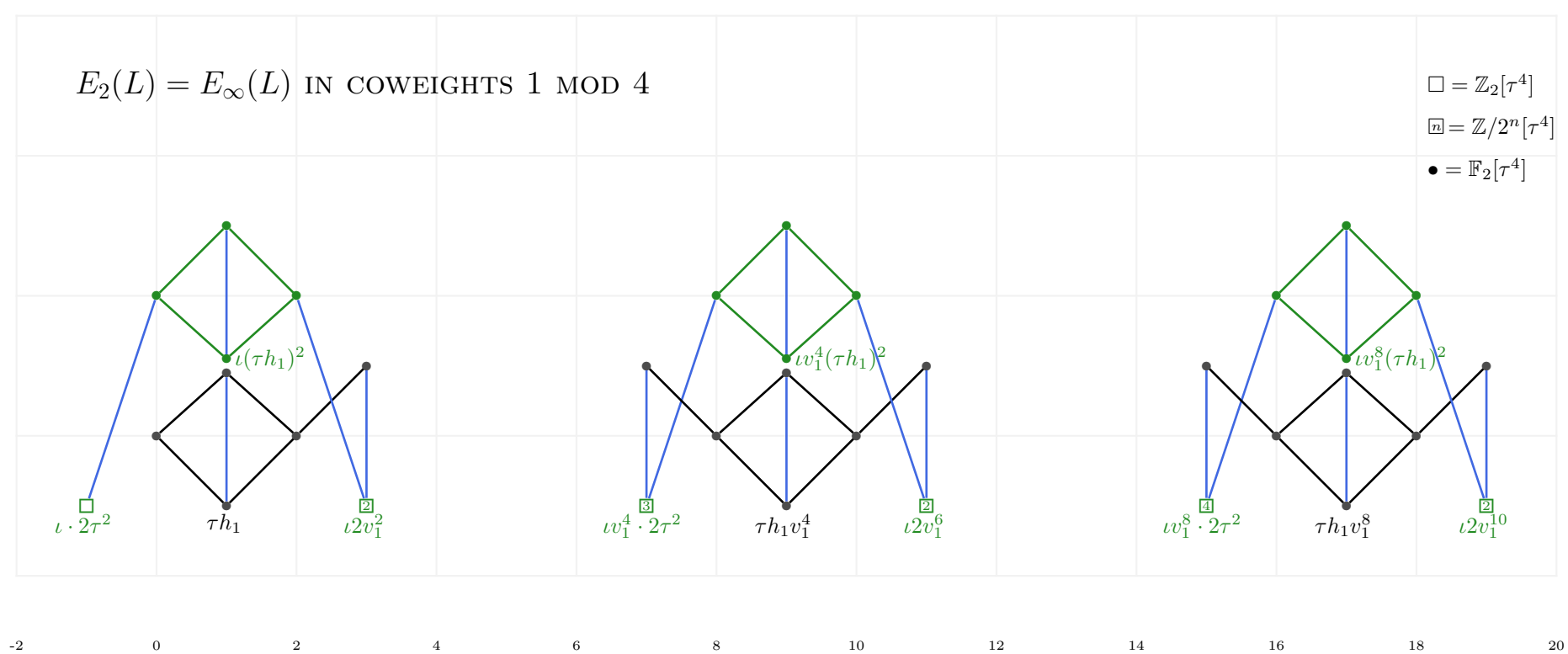


FIGURE 14. The E_∞ -page of the effective spectral sequence for L in coweights 1 mod 4

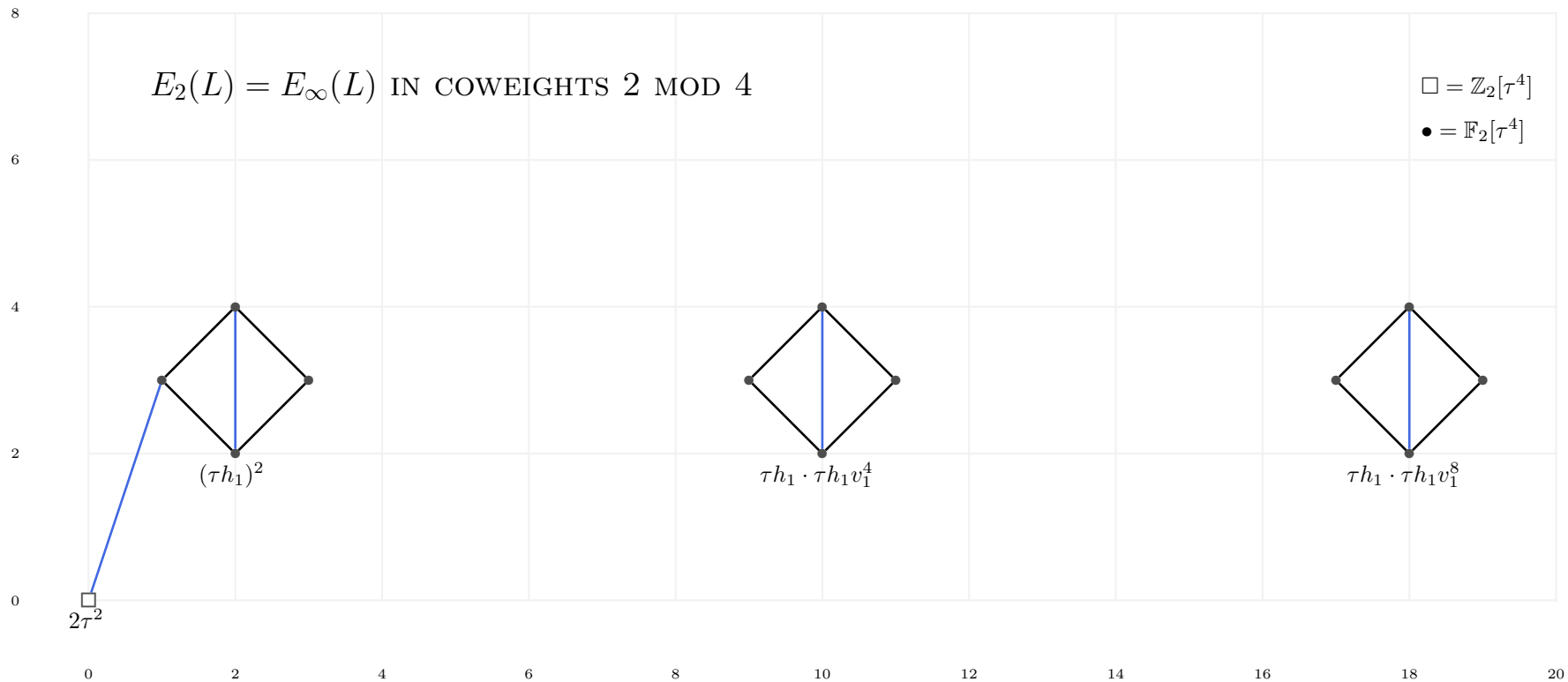


FIGURE 15. The E_∞ -page of the effective spectral sequence for L in coweights 2 mod 4

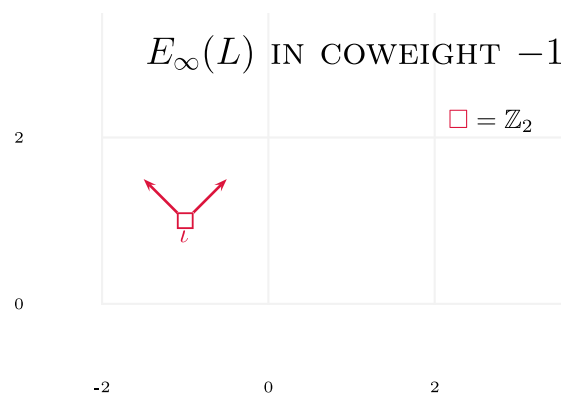


FIGURE 16. The E_∞ -page of the effective spectral sequence for L in coweight -1

$E_\infty(L)$ IN COWEIGHTS 3 MOD 8

- $\square = \mathbb{Z}_2[\tau^8]$
- $\boxed{n} = \mathbb{Z}/2^n[\tau^8]$
- $\bullet = \mathbb{F}_2[\tau^8]$

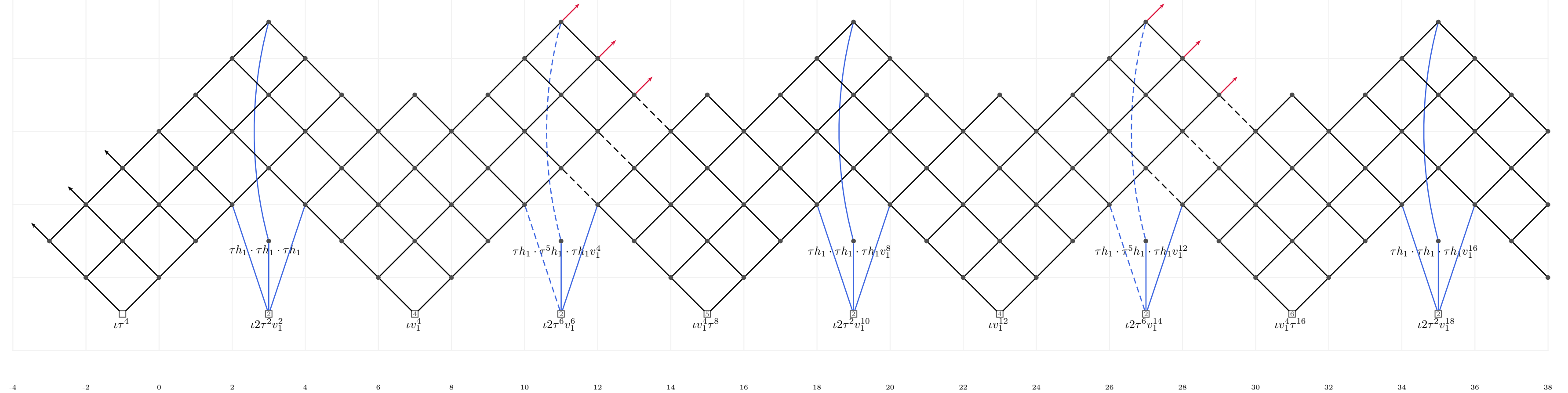


FIGURE 17. The E_∞ -page of the effective spectral sequence for L in coweights 3 mod 8

$E_\infty(L)$ IN COWEIGHTS 7 MOD 16

- $\square = \mathbb{Z}_2[\tau^{16}]$
- $\boxplus = \mathbb{Z}/2^n[\tau^{16}]$
- $\bullet = \mathbb{F}_2[\tau^{16}]$

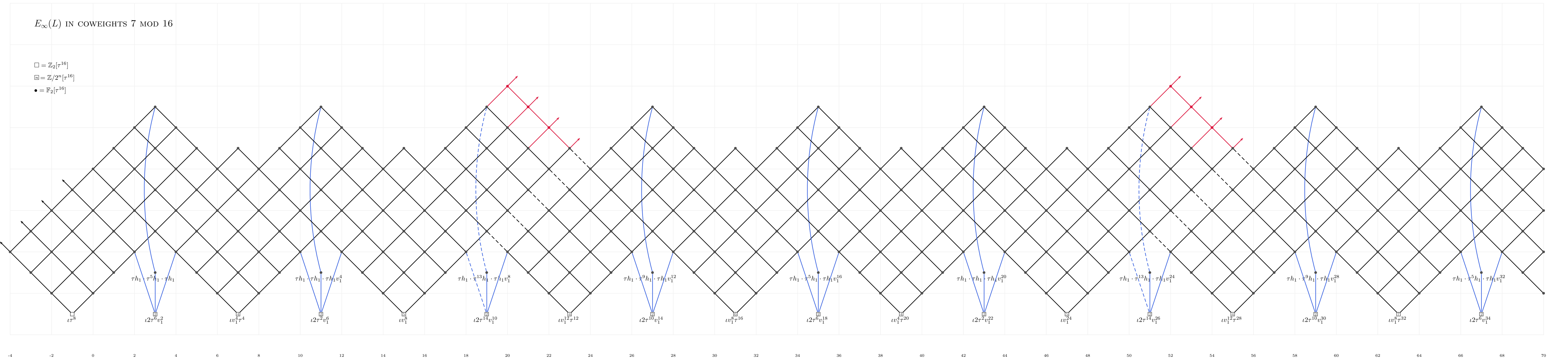
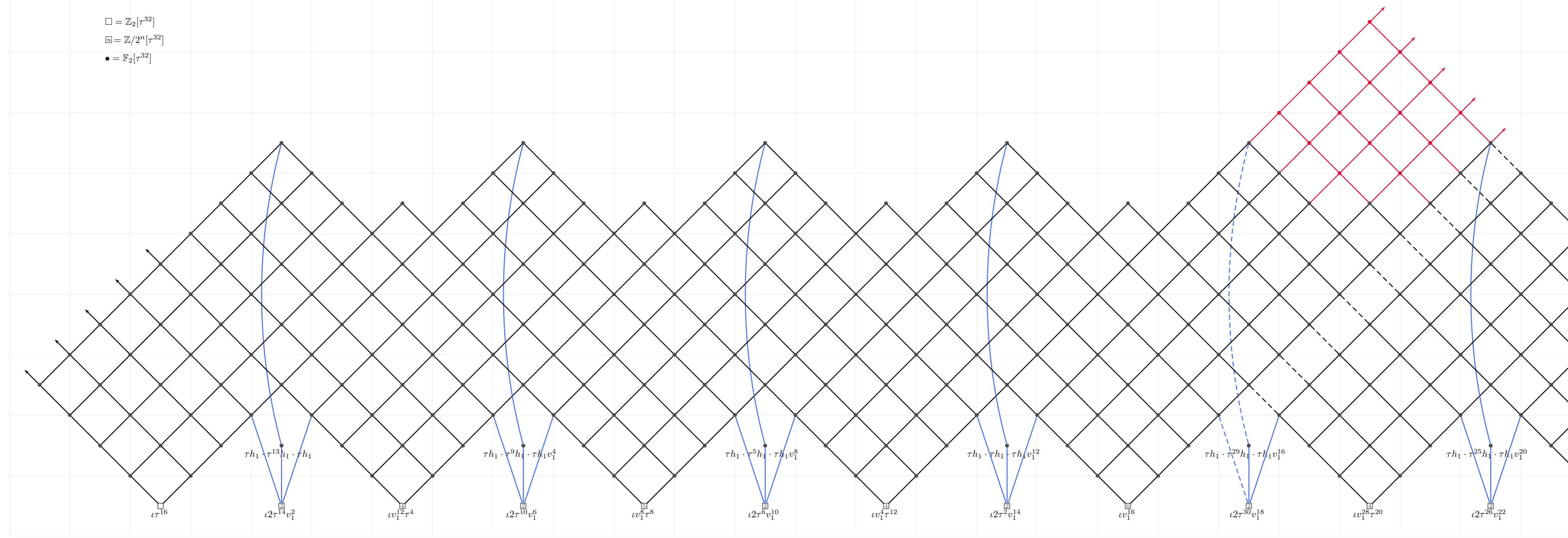


FIGURE 18. The E_∞ -page of the effective spectral sequence for L in coweights 7 mod 16

$E_\infty(L)$ IN COWEIGHTS 15 MOD 32

18
16
14
12
10
8
6
4
2
0

- $\square = \mathbb{Z}_2[\tau^{32}]$
- $\boxplus = \mathbb{Z}/2^n[\tau^{32}]$
- $\bullet = \mathbb{F}_2[\tau^{32}]$



-6 -4 -2 0 2 4 6 8 10 12 14 16 18 20 22 24 26 28 30 32 34 36 38 40 42 44 46

FIGURE 19. The E_∞ -page of the effective spectral sequence for L in coweights 15 mod 32

REFERENCES

- [AM17] Michael Andrews and Haynes Miller. Inverting the Hopf map. *J. Topol.*, 10(4):1145–1168, 2017.
- [ARØ20] Alexey Ananyevskiy, Oliver Röndigs, and Paul Arne Østvær. On very effective hermitian K-theory. *Mathematische Zeitschrift*, 294(3):1021–1034, 2020.
- [Bac18] Tom Bachmann. Motivic and real étale stable homotopy theory. *Compositio Mathematica*, 154(5):883–917, Mar 2018.
- [Bal21] William Balderrama. The Borel C_2 -equivariant $K(1)$ -local sphere. *arXiv:2103.13895*, 2021.
- [BG121] Eva Belmont, Bertrand J. Guillou, and Daniel C. Isaksen. C_2 -equivariant and \mathbb{R} -motivic stable stems II. *Proc. Amer. Math. Soc.*, 149(1):53–61, 2021.
- [BH20] Tom Bachmann and Michael J. Hopkins. η -periodic motivic stable homotopy theory over fields. *arxiv 2005.06778*, 2020.
- [BI20] Eva Belmont and Daniel C. Isaksen. \mathbb{R} -motivic stable stems. *arXiv:2001.03606*, 2020.
- [Boa99] J. Michael Boardman. Conditionally convergent spectral sequences. *Contemporary Mathematics*, 239:49–84, 1999.
- [BR21] Robert R. Bruner and John Rognes. The Adams spectral sequence for the image-of- J spectrum. *arXiv:2105.02601*, 2021.
- [BS20] Mark Behrens and Jay Shah. C_2 -equivariant stable homotopy from real motivic stable homotopy. *Ann. K-Theory*, 5(3):411–464, 2020.
- [Car19] Christian Carrick. Smashing localizations in equivariant stable homotopy. *arXiv:1909.08771*, 2019.
- [Dav75] Donald M. Davis. The cohomology of the spectrum bJ . *Bol. Soc. Mat. Mexicana (2)*, 20(1):6–11, 1975.
- [DI17] Daniel Dugger and Daniel C. Isaksen. Low-dimensional Milnor-Witt stems over \mathbb{R} . *Ann. K-Theory*, 2(2):175–210, 2017.
- [GI16] Bertrand Guillou and Daniel C. Isaksen. The η -inverted \mathbb{R} -motivic sphere. *Algebraic & Geometric Topology*, 16(5):3005–3027, 2016.
- [Hil11] Michael A. Hill. Ext and the motivic Steenrod algebra over \mathbb{R} . *J. Pure Appl. Algebra*, 215(5):715–727, 2011.
- [HKO11] Po Hu, Igor Kriz, and Kyle Ormsby. Convergence of the motivic Adams spectral sequence. *Journal of K-theory: K-theory and its Applications to Algebra, Geometry, and Topology*, 7:573 – 596, 06 2011.
- [IS11] Daniel C. Isaksen and Armira Shkembli. Motivic connective K -theories and the cohomology of $A(1)$. *J. K-Theory*, 7(3):619–661, 2011.
- [Isa19] Daniel C. Isaksen. Stable stems. *Mem. Amer. Math. Soc.*, 262(1269):viii+159, 2019.
- [Kon21] Hana Jia Kong. The C_2 -effective spectral sequence for C_2 -equivariant connective real K -theory. *arXiv:2004.00806*, 2021.
- [Lev13] Marc Levine. Convergence of Voevodsky’s slice tower. *Doc. Math.*, 18:907–941, 2013.
- [Lev15] Marc Levine. The Adams–Novikov spectral sequence and Voevodsky’s slice tower. *Geom. Topol.*, 19(5):2691–2740, 2015.
- [Mor04] Fabien Morel. On the motivic π_0 of the sphere spectrum. In *Axiomatic, enriched and motivic homotopy theory*, volume 131 of *NATO Sci. Ser. II Math. Phys. Chem.*, pages 219–260. Kluwer Acad. Publ., Dordrecht, 2004.
- [OR20] Kyle Ormsby and Oliver Röndigs. The homotopy groups of the η -periodic motivic sphere spectrum. *Pacific J. Math.*, 306(2):679–697, 2020.
- [RSØ19] Oliver Röndigs, Markus Spitzweck, and Paul Arne Østvær. The first stable homotopy groups of motivic spheres. *Ann. of Math. (2)*, 189(1):1–74, 2019.
- [SØ12] Markus Spitzweck and Paul Arne Østvær. Motivic twisted K -theory. *Algebraic & Geometric Topology*, 12(1):565–599, 2012.
- [Spi08] Markus Spitzweck. Relations between slices and quotients of the algebraic cobordism spectrum. *Homology, Homotopy and Applications*, 12:335–351, 2008.
- [Voe02] Vladimir Voevodsky. Open problems in the motivic stable homotopy theory. i. *Motives, polylogarithms and Hodge theory, Part I (Irvine, CA, 1998)*, 3:3–34, 2002.
- [Wil18] Glen Matthew Wilson. The eta-inverted sphere over the rationals. *Algebr. Geom. Topol.*, 18(3):1857–1881, 2018.

DEPARTMENT OF MATHEMATICS, UNIVERSITY OF CALIFORNIA SAN DIEGO, LA JOLLA, CA 92093, USA
Email address: `ebelmont@ucsd.edu`

DEPARTMENT OF MATHEMATICS, WAYNE STATE UNIVERSITY, DETROIT, MI 48202, USA
Email address: `isaksen@wayne.edu`

SCHOOL OF MATHEMATICS, INSTITUTE FOR ADVANCED STUDY, PRINCETON, NJ 08540, USA
Email address: `hana.jia.kong@gmail.com`